AD-A115 317 CALSPAN ADVANCED TECHNOLOGY CENTER BUFFALO NY AERODYN--ETC F/G 19/1
NUMERICAL MODEL FOR FLUID SPIN-UP IN A PARTIALLY-FILLED CYLINDE--ETC(U)
MAY 82 G F HOMICZ DAAG29-81-C-0007
UNCLASSIFIED CALSPAN-6856-A-1 NL

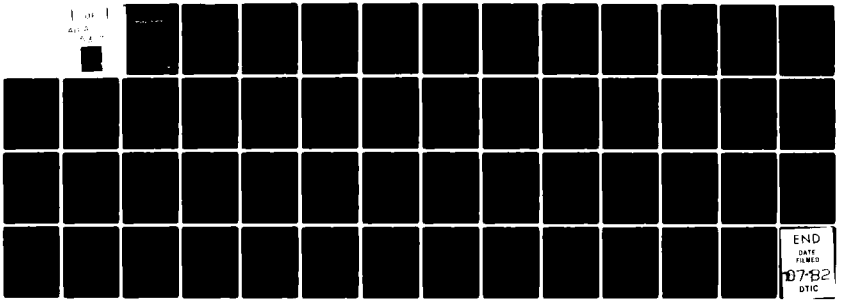

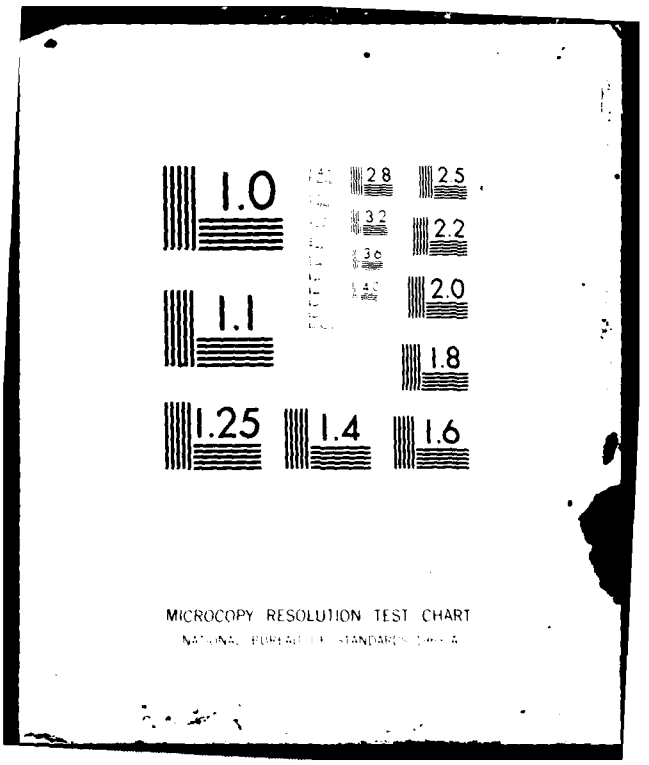
1.0
1.1
1.25
1.4
1.6
1.8
2.0
2.2
2.5
2.8
3.2
3.6
4.0
MICROCOPY RESOLUTION TEST CHART

ARO-17747.1-EG

(12)

ARVIN/CALSPAN

NUMERICAL MODEL FOR FLUID SPIN-UP IN A PARTIALLY-FILLED CYLINDER

INTERIM TECHNICAL REPORT

Calspan Report No. 6856-A-1

Gregory F. Homicz

May 1982

Prepared For:
U.S. ARMY RESEARCH OFFICE

CONTRACT NO. DAAG29-81-C-0007

Prepared By:

Calspan Advanced Technology Center
Aerodynamic Research Department
P.O. Box 400
Buffalo, NY 14225

**APPROVED FOR PUBLIC RELEASE;
DISTRIBUTION UNLIMITED.**

The view, opinions, and/or findings contained in this report are those of the author(s) and should not be construed as an official Department of the Army position, policy, or decision, unless so designated by other documentation.

UNCLASSIFIED

SECURITY CLASSIFICATION OF THIS PAGE (When Data Entered)

REPORT DOCUMENTATION PAGE	READ INSTRUCTIONS BEFORE COMPLETING FORM
1. REPORT NUMBER / 2. GOVT ACCESSION NO. AD-A115 317	3. RECIPIENT'S CATALOG NUMBER
4. TITLE (and Subtitle) NUMERICAL MODEL FOR FLUID SPIN-UP IN A PARTIALLY-FILLED CYLINDER	5. TYPE OF REPORT & PERIOD COVERED Interim Technical Report 3/1/81 - 2/28/82
	6. PERFORMING ORG. REPORT NUMBER 6856-A-1
7. AUTHOR(s) Gregory F. Homicz	8. CONTRACT OR GRANT NUMBER(s) DAAG29-81-C-0007
9. PERFORMING ORGANIZATION NAME AND ADDRESS Calspan Advanced Technology Center P. O. Box 400 Buffalo, New York 14225	10. PROGRAM ELEMENT, PROJECT, TASK AREA & WORK UNIT NUMBERS
11. CONTROLLING OFFICE NAME AND ADDRESS U.S. Army Research Office Post Office Box 12211 Research Triangle Park, NC 27709	12. REPORT DATE May 1982
	13. NUMBER OF PAGES 46
14. MONITORING AGENCY NAME & ADDRESS(if different from Controlling Office)	15. SECURITY CLASS. (of this report) UNCLASSIFIED
	15a. DECLASSIFICATION/DOWNGRADING SCHEDULE

16. DISTRIBUTION STATEMENT (of this Report)

Approved for public release; distribution unlimited.

17. DISTRIBUTION STATEMENT (of the abstract entered in Block 20, if different from Report)

18. SUPPLEMENTARY NOTES

The view, opinions and/or findings contained in this report are those of the author(s) and should not be construed as an official Department of the Army position, policy, or decision, unless so designated by other documentation.

19. KEY WORDS (Continue on reverse side if necessary and identify by block number)

Rotating Flow
Liquid-Filled Shells
Spin-Up

20. ABSTRACT (Continue on reverse side if necessary and identify by block number)

A theoretical investigation is presented for the axisymmetric spin-up of fluid in a partially-filled cylindrical cavity. It is an extension of the earlier analyses of Wedemeyer, and of Goller and Ranov, to those cases where the liquid free surface intersects one or both endwalls. The simplifying assumptions of a columnar flow and the quasi-steady treatment of the Ekman layer pumping of the secondary flow are retained. Earlier estimates of the Ekman layer pumping are modified heuristically for situations where the layer(s) no longer

DD FORM 1 JAN 73 1473

UNCLASSIFIED

SECURITY CLASSIFICATION OF THIS PAGE (When Data Entered)

20. (Cont'd)

covers the entire wall. Also, due to the very steep free surface contour in the latter stages of spin-up, it was found advantageous to develop the free surface equations in an axial, rather than radial, coordinate frame.

Using a straightforward finite-difference algorithm, a computer program was developed which predicts the azimuthal velocity profile and free surface contour as functions of time. The fluid angular momentum exhibits a simple exponential behavior in time. For Reynolds numbers in the range 10^4-10^5, the growth rate appears uniform up to the point where the bottom endwall is intersected; after this, exponential behavior is still displayed, but at a reduced rate. For Reynolds number on the order of 10^3, a uniform growth rate is exhibited over the whole of the calculation. The predictions of the present analysis should prove useful as input to the calculation of the spin-decay of liquid filled projectiles, and the eigenfrequencies of the perturbed fluid motion, both of which are of critical importance in determining the projectile's stability.

FOREWORD

This interim report documents the results of the first year of the theoretical program "Numerical Models for Fluid Behavior During Spin-Up in Liquid-Filled Shells" sponsored by the U.S. Army Research Office under Contract No. DAAG29-81-C-0007. The program is under the technical supervision of Dr. Robert E. Singleton. Recognition is due Dr. Raymond S. Sedney and Mr. Nathan Gerber of the Launch and Flight Division, U.S. Army Ballistic Research Laboratory, who through their technical discussions with the author have had a significant impact on the course of this work. The implicit computer code which they provided, and which formed the basis for that developed here, is also gratefully acknowledged. Finally, the author wishes to thank his colleague, Dr. William J. Rae, for his advice and encouragement.

TABLE OF CONTENTS

LIST OF ILLUSTRATIONS

LIST OF TABLES

Section 1
INTRODUCTION

The goal of the theoretical investigation described here is to obtain a clearer understanding of the fluid dynamics of liquid-filled shells for those cases where the fluid only partially fills its cavity. Problems can arise during the flight of such projectiles when there is a strong coupling between the perturbed motion of the rapidly spinning shell casing and the attendant wave motion excited in the fluid. In addition, unlike a solid filler which always rotates with the same angular velocity as the casing, the liquid filler will rotate at a reduced angular velocity over much of the trajectory. The result is a net transfer of angular momentum from casing to fluid, which in itself can be destabilizing.[1] Considerations of internal fluid motion also play an important role in spin-stabilized liquid propellant rockets.[2]

The model problem most often studied by investigators is the axisymmetric spin-up of fluid in a right circular cylinder. We seek to represent the evolution with time of the fluid motion, particularly the azimuthal velocity, as it asymptotically approaches solid-body rotation. Such a calculation is necessary as input for the prediction of the spin decay of liquid-filled projectiles.[3,4] It can also serve as the base flow about which to carry out a perturbation analysis of the eigenfrequencies of the fluid.[5,6] The latter are of critical importance to the question of the stability of the fluid-shell system.[1]

Most previous investigations of the problem have assumed the cylinder to be completely filled. The earliest work appears to be that of McLeod,[7] who assumed

---

1. Engineering Design Handbook. Liquid-Filled Projectile Design, AMC Pamphlet No. 706-165, U.S. Army Materiel Command, Washington, D.C., April 1969.
2. Winch, D.M., An Investigation of the Liquid Level at the Wall of a Spinning Tank, NASA TN D-1536, August 1962.
3. Kitchens, C.W., Jr., Gerber, N. and Sedney, R., "Spin Decay of Liquid Filled Projectiles," J. of Spacecraft, Vol. 15, No. 6, 348-354, December 1978.
4. Kitchens, C.W., Jr. and Gerber, N., Prediction of Spin Decay of Liquid Filled Projectiles, BRL Report 1996, Aberdeen Proving Ground, Md., July 1977.
5. Kitchens, C.W., Jr., Gerber, N., and Sedney, R., Oscillations of a Liquid in a Rotating Cylinder: Part I. Solid-Body Rotation, ARBRL-TR-02081, Aberdeen Proving Ground, Md., June 1978.
6. Kitchens, C.W., Jr., Gerber, N., and Sedney, R., Oscillations of a Liquid in a Rotating Cylinder: Part II. Spin-Up, BRL Report (in preparation).
7. McLeod, A.R., "The Unsteady Motion Produced in a Uniformly Rotating Cylinder of Water by a Sudden Change in the Angular Velocity of the Boundary", Philosophical Magazine and Journal of Science, Vol. 44, No. 259, 1-14, 1922.

that viscous diffusion was the dominant spin-up mechanism, and so neglected the nonlinear convective terms in the equations. Winch[2] later extended McLeod's arguments to the case where a free surface was present. In both cases the theory significantly overestimated the fluid spin-up time. Greenspan, et al.[8,9] considered the situation in which $Re = \Omega R^2/\nu$ is large, which is typical for the cases of interest here. Convective terms were retained, but in the limit where only small changes in rotational speed were allowed, i.e., small Rossby number, $\epsilon = \Delta\Omega/\Omega$. The latter served as the expansion parameter for a small perturbation analysis of the problem. It was found that the Ekman layers on the endwalls drive a strong secondary flow which accelerates the spin-up process. The characteristic spin-up time was shown to scale as $t_s \sim \frac{H}{R} Re^{1/2} \Omega^{-1}$.

Wedemeyer[10] was the first to carry out a nonlinear analysis of this problem which did not hinge on the Rossby number being small. He argued that the direct influence of viscosity was likely to be felt only in the Ekman layers. The bulk of the flow in the interior, or core flow as he called it, was thus assumed to be inviscid. Further, the radial and axial flow velocities, $\bar{u}$ and $\bar{w}$, would be expected to be much smaller than the azimuthal component, $\bar{v}$, in this region. He also assumed, based on Benton's[11] work, that the Ekman layer structure would accommodate itself in a quasi-steady fashion to changes in the core flow. With these approximations, the Navier-Stokes equations reduce to a single nonlinear partial differential equation for $\bar{v}$ as a function of $\bar{r}$ and $\bar{t}$, which has a simple closed form solution for the case of impulsive spin-up from rest.

Wedemeyer's phenomenological analysis formed the groundwork for several amplifications and extensions.[12-16] Briefly, the qualitative picture that emerges

---

8. Greenspan, H.P. and Howard, L.N., "On a Time-Dependent Motion of a Rotating Fluid," J. of Fluid Mechanics, Vol. 17 Pt. 3, 385-404, 1963.
9. Greenspan, H.P. and Weinbaum, S., "On Non-Linear Spin-Up of a Rotating Fluid," J. of Mathematics and Physics, Vol. 44, 66-85, 1965.
10. Wedemeyer, E.H., "The Unsteady Flow Within a Spinning Cylinder," J. of Fluid Mechanics, Vol. 20 Pt. 3, 383-399, 1964.
11. Benton, E.R., "On the Flow Due to a Rotating Disk," J. of Fluid Mechanics, Vol. 24 Pt. 4, 781-800, 1966.
12. Benton, E.R., "Vorticity Dynamics in Spin-Up from Rest", Physics of Fluids, Vol. 22 No. 7, 1250-1251, 1979.
13. Venezian, G., "Non-Linear Spin-Up", Topics in Ocean Engineering, Vol. 2, 87-96, Gulf Publishing Co., Houston, 1970.
14. Weidman, P.D., "On the Spin-Up and Spin-Down of a Rotating Fluid. Part I: Extending the Wedemeyer Model. Part II: Measurements and Stability", J. of Fluid Mechanics, Vol. 77 Pt. 4, 685-735, 1976.

is as follows. Due to the no-slip boundary condition, the fluid motion in the Ekman layer closely follows that of the wall beneath it. Thus, when the cylinder is impulsively started, this fluid is flung out toward the sidewall by centrifugal forces; the radial pressure gradient needed to prevent such a flux has not yet had time to develop, since it is determined by the still more or less quiescent core flow. Since fluid volume must be conserved, this outward flux in the Ekman layer must be balanced by an influx of fluid from the core flow. The Ekman layer thus provides a pumping action on the interior flow. Near the cylindrical axis fluid is sucked into the viscous layer where it acquires additional angular momentum, is flung outward, and then turned back into the core flow to complete the circuit.

Hence a strong secondary flow is set up. The core flow is characterized by a (suitably normalized) azimuthal velocity profile, v, of order one, and a radial velocity, u, of order $(R/H)Re^{-1/2}$, which is directed in toward the axis. The strong rotational effects in this flow allow application of the Taylor-Proudman theorem,[17] which indicates that u and v are both independent of z to this approximation. On the other hand, the axial velocity, w, varies linearly from zero at the mid-plane to a maximum value at the endwall, where it is accommodated to the wall through the Ekman layer structure. It is found that w also changes sign between the axis and the sidewall to reflect the sink/source nature of the matching with the Ekman layer.

Thus, while viscosity is responsible for transmitting angular momentum from the cylinder to the fluid in the Ekman layer, it is the inviscid core that is responsible for redistributing it over the rest of the flow. It should be noted that the characteristic viscous diffusion time, t_D, scales as $O(R^2/\nu) = Re\,\Omega^{-1}$, and hence $\Omega^{-1} \ll t_s \ll t_D$. The fluid is seen to achieve solid-body rotation on a much shorter time scale than t_D; hence it really is the secondary flow and not viscous diffusion alone that is responsible for spin-up, as evidenced by the poor correlation of the analyses of McLeod[7] and Winch[2] with experiment.

---

15. Watkins, W.B. and Hussey, R.G., "Spin-Up from Rest: Limitations of the Wedemeyer Model", Physics of Fluids, Vol. 16 No. 9, 1530-1531, 1973.
16. Watkins, W.B. and Hussey, R.G., "Spin-Up from Rest in a Cylinder", Physics of Fluids, Vol. 20 No. 10, 1596-1604, 1977.
17. Greenspan, H.P., The Theory of Rotating Fluids, Cambridge University Press, London, 1968.

Recent advances in computer hardware and algorithms have made it feasible to attack this problem from first principles. Thus Warn-Varnas, et al.,[18] and Kitchens[19,20] have each solved the full unsteady, axisymmetric Navier Stokes equations for the spin-up of a viscous incompressible fluid in a completely filled cylinder, using finite-difference techniques. Their calculations agree with one another, and with laboratory experiments. They further reinforce the qualitative picture described above based on the partly phenomenological Wedemeyer model.

The investigations discussed above, with the exception of that by Winch,[2] were all concerned with the case where the liquid completely fills the cavity. In practice, however, the shells are often only partially filled. Moreover, field data[21] show that the probability of a projectile experiencing an erratic flight is a strong function of its fill ratio, i.e., the percentage of the cavity volume occupied by fluid. Thus there is an important need to understand the influence of the interior free surface on the spin-up process.

Gerber[22,23] has shown that the final form of this surface, after solid-body rotation is achieved, is a parabola whose shape is determined by the fill ratio and the Froude number, $F = (\Omega R)^2/gH$. Winch's[2] attempt to predict the evolution of this shape with time failed because he neglected the dominant secondary flow. Goller and Ranov[24] have extended Wedemeyer's model to include the free surface motion, and were able to show that it acts to retard the spin-up process. They presented numerical results for both the free surface shape and the azimuthal velocity profile as functions

---

18. Warn-Varnas, A., Fowlis, W.W., Piacsek, S., and Lee, S.M., "Numerical Solutions and Laser-Doppler Measurements of Spin-Up", J. of Fluid Mechanics, Vol. 85 Pt. 4, 609-639, 1978.
19. Kitchens, C.W., Jr., Navier-Stokes Solutions for Spin-Up from Rest in a Cylindrical Container, ARBRL-TR-02193, Aberdeen Proving Ground, Md., September 1979.
20. Kitchens, C.W., Jr., Navier-Stokes Solutions for Spin-Up by a Predictor Corrector Multiple-Iteration Method, AIAA Paper No. 79-1454, presented at AIAA Computational Fluid Dynamics Conference, July 23-25, 1979, Williamsburg, Va.
21. Mark, A., Measurements of Angular Momentum Transfer in Liquid-Filled Projectiles, ARBRL-TR-2029, Aberdeen Proving Ground, Md., November 1977.
22. Gerber, N., "Properties of Rigidly Rotating Liquids in Closed Partially Filled Cylinders", ASME Transactions, J. of Applied Mechanics, Vol. 97, 734-735, 1975.
23. Gerber, N., Rigidly Rotating Liquids in Closed Partially Filled Cylindrical Cavities, BRL-MR-2462, Aberdeen Proving Ground, Md., March 1975.
24. Goller, H. and Ranov, T., "Unsteady Rotating Flow in a Cylinder with a Free Surface", ASME Transactions, J. of Basic Engineering, Vol. 90D, No. 4, 445-454, December 1968.

of time. The former were compared with data from a series of laboratory experiments and the agreement was quite good. The problem with applying their analysis to actual configurations is that Goller and Ranov assumed the free surface did not intersect either of the endwalls. This is a rather restrictive assumption, as shown by the analysis of Gerber.[22,23] The purpose of the investigation reported here is to extend the Wedemeyer-Goller-Ranov model to situations where the free surface intersects one or both of the endwalls.

The analysis is described in Section 2, and numerical results are presented and discussed in Section 3. The conclusions drawn are summarized in Section 4. To help preserve continuity in the main text, the equations describing the free surface motion are developed in Appendix A and called out as needed. Appendix B provides some details on the finite difference algorithm used in solving the equations.

Section 2
ANALYSIS

We wish to predict the spin-up of fluid in a cylinder of radius R and height H (see Figure 1) which at t = 0 impulsively begins to spin with constant angular velocity, Ω , about its axis. The fluid is incompressible and characterized by its density, ρ , and kinematic viscosity, ν . Its initial level when at rest is denoted by L. The velocity components in the $(\bar{r}, \Theta, \bar{z})$ coordinates are $(\bar{u}, \bar{v}, \bar{w})$ respectively.

The fluid motion is governed by the axisymmetric Navier-Stokes equations. However, following Wedemeyer,[10] the motion in the core flow is assumed to be predominantly rotational in nature, so that terms involving $\bar{u}$ and $\bar{w}$ are neglected. This leads to a Taylor-Proudman type flow, i.e., to this degree of approximation $\bar{u}$, $\bar{v}$ and $\bar{p}$ are functions of only $\bar{r}$ and $\bar{t}$. After converting to dimensionless variables (see Nomenclature list), the equation for v (r, t) reduces to,

$$\frac{\partial v}{\partial t} + u\left(\frac{\partial v}{\partial r} + \frac{v}{r}\right) = Re^{-1}\left[\frac{\partial^2 v}{\partial r^2} + \frac{\partial}{\partial r}\left(\frac{v}{r}\right)\right] \tag{1}$$

subject to the initial and boundary conditions,

$$v(r, 0) = 0 \qquad 0 \leq r \leq 1 \tag{2a}$$
$$v(0, t) = 0 \qquad t > 0 \tag{2b}$$
$$v(1, t) = 1 \qquad t > 0 \tag{2c}$$

An additional expression relating u to v is required to close the system. Assuming for the moment that this is known, we proceed to form a finite difference analog to Eq. (1), using a uniform grid in space and time. Thus, we define $r_j = (j-1)\ \Delta r$, $j = 1,2 \ldots NJ$ where $\Delta r = 1/(NJ-1)$. Then denoting $v(r_j, t = i\ \Delta t)$ by v^i_j , we can express the solution at the next time step by

$$v_j^{i+1} = v_j^i + \frac{\Delta t}{2}\left[G^i(u, v) + G^{i+1}(u, v)\right] + O(\Delta t)^3 \tag{3a}$$

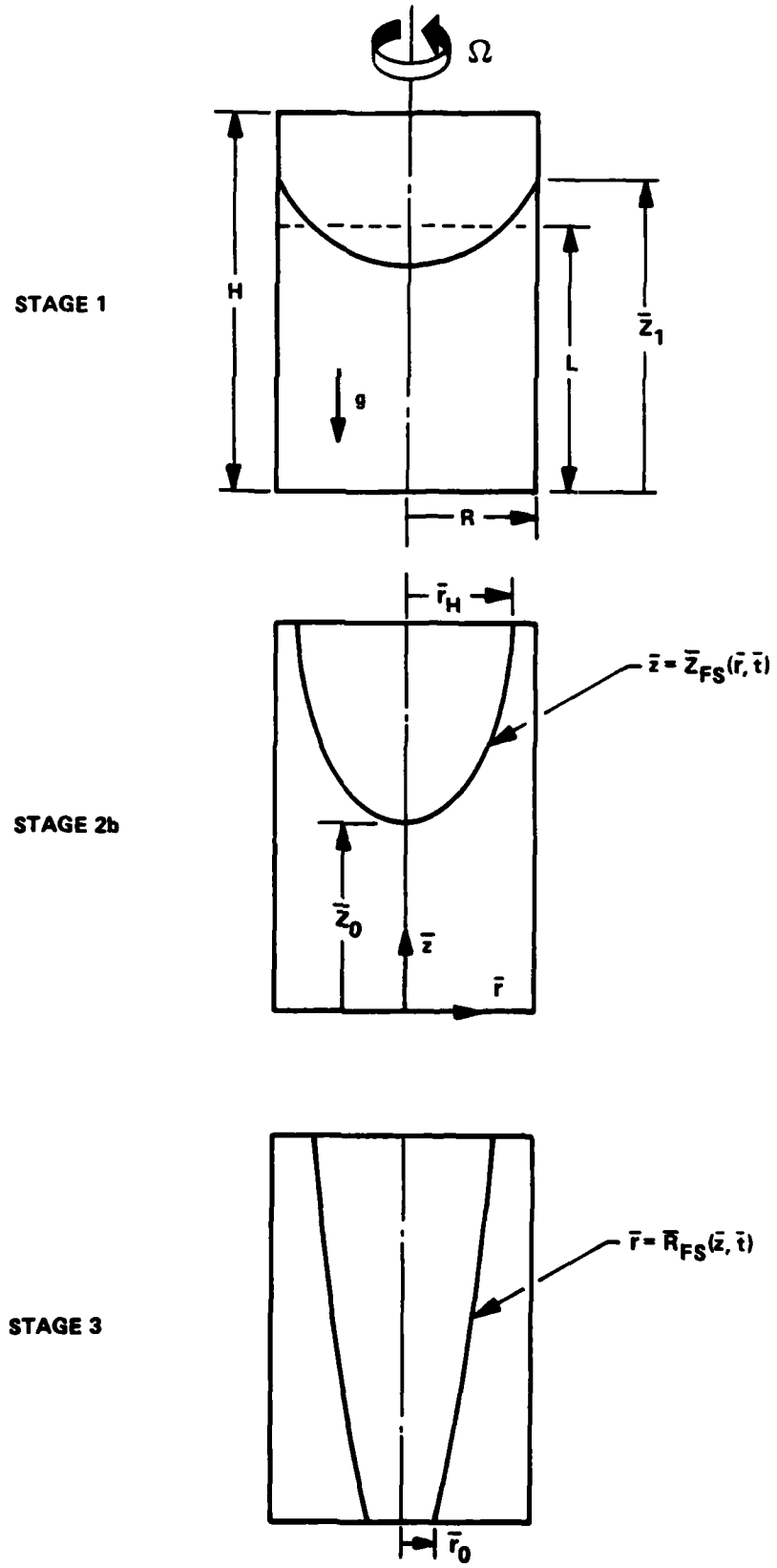

Figure 1 CYLINDRICAL GEOMETRY AND POSSIBLE FLUID CONFIGURATIONS FOR L/H ≥ ½

where

$$G^i(u,v) = Re^{-1}\left[\frac{\partial^2 v^i}{\partial r^2} + \frac{\partial}{\partial r}\left(\frac{v^i}{r}\right)\right] - u^i\left(\frac{\partial v^i}{\partial r} + \frac{v^i}{r}\right) \qquad (3b)$$

and from Eq. (2b, c)

$$v_1^i = 0 \qquad (4a)$$

$$v_{NJ}^i = 1 \qquad (4b)$$

Centered second-order accurate differences are used to approximate the spatial derivatives in Eq. (3b). When assembled into Eq. (3a), the right-hand side will contain v_{j-1}^{i+1}, v_j^{i+1}, and v_{j+1}^{i+1}. Thus the system is implicit in that all velocity values at the new time step must be solved for *simultaneously*. It is also tridiagonal, and so lends itself to solution by the efficient Thomas algorithm;[25] the details are given in Appendix B. An implicit scheme offers the advantage of using time steps which are ordinarily larger than would be allowed by an explicit scheme, such as that used by Goller and Ranov.[24]

The presence of u in Eq. (3b) represents a nonlinearity, which is handled via an iterative relaxation procedure. The distributions v_j^{i-1} and v_j^i are presumed known, and by linear extrapolation a first guess is made for v_j^{i+1}. From this, an estimate of u_j^{i+1} is made, and then Eq. (3) is solved. If at each point this solution agrees with that which was estimated to within some prescribed relative error, it is accepted and all variables are updated in anticipation of the next time step. If they do not agree, the solution is relaxed as follows

$$v_j^{(m+1)} = \alpha v_j^s + (1-\alpha) v_j^{(m)} \qquad (5)$$

where $v_j^{(m)}$ represents the mth iterate to v_j^{i+1}, and v_j^s represents the solution vector to Eq. (3) based on this iterate. This is repeated until the desired convergence is achieved. It was found necessary to vary the relaxation parameter, α, during the course of the calculation to insure convergence. The values used are given in Appendix B.

---

25. Richtmeyer, R.D. and Morton, K.W., Difference Methods for Initial Value Problems, 2nd Ed., Chapter 8, Interscience Publishers, New York, 1967.

The above discussion presumes the existence of a relation determining u(r, t) as a function of v(r, t). For the fully-filled cylinder, Wedemeyer argued that to preserve continuity the radially outward flux in the endwall Ekman layers must be balanced at each radius by an equal but opposite inward flux in the core flow. Further, Benton[11] had shown that the Ekman layer flow established itself on a time scale of the order of a few revolutions of the cylinder, which is orders of magnitude faster than the interior fluid spin-up time. Hence the efflux in the layers was assumed to accommodate itself in a quasi-steady manner to changes in the core flow. Due to the columnar nature of the motion the radial influx in the core is spread uniformly with depth. This led Wedemeyer to the following, as he called it, compatibility condition relating u(r, t) to v(r, t):

$$u = -0.886 \left(\frac{R}{H}\right) Re^{-1/2} (r - v) \tag{6}$$

For a partially-filled cylinder, there is an additional contribution to u resulting from the free surface motion. The drop in fluid level near the axis and the accompanying rise at the sidewall imply a radial outflux in opposition to the influx generated by the Ekman layers. Further, these layers will no longer necessarily cover the entire endwall. These features of the flow serve to retard the spin-up process. For convenience we separate the contributions to u from the top and bottom Ekman layers and the free surface motion as follows,

$$u = u_{TEL} + u_{BEL} + u_{FS} \tag{7}$$

The form each of these will take at any instant depends on whether the free surface intersects neither, the top, or both of the endwalls. Following Gerber,[22,23] we shall refer to these successive configurations as Stages 1, 2b, and 3 as indicated in Figure 1.* The remaining discussion naturally divides itself along the same lines.

---

* Gerber also treated a fourth configuration, Stage 2a, in which the free surface intersects the bottom, but not the top, endwall. This occurs only for fill ratios, L/H, less than one-half. Such cases are not considered here, although the extension of the present methods to flows in Stage 2a should be straightforward.

Stage 1

This is the case treated previously by Goller and Ranov,[24] in which neither endwall is intersected. Before u can be found, one must first determine the free surface contour, $Z_{FS}(r,t)$, given v(r,t). This is done using Eqs. (A-3) and (A-5) from Appendix A,

$$\bar{Z}_1(t) = \frac{L}{H} + F\int_0^1 v^2\, r\, dr \tag{8a}$$

$$\bar{Z}_{FS}(r,t) = \bar{Z}_1 - F\int_r^1 \frac{v^2}{r'}\, dr' \tag{8b}$$

Simpson's rule is used to evaluate the quadatures on the radial grid.

Clearly for this stage, $u_{TEL} = 0$. The bottom Ekman layer, however, is assumed to pump fluid at the same rate as for the fully filled case. But whereas before the compensating flux in the core flow was spread uniformly over half the cylinder height (by symmetry), it is now spread over the fluid depth, Z_{FS}:

$$2\pi \bar{r}\, \bar{Z}_{FS}\, \bar{u}_{BEL} = -2\pi \bar{r}\int_0^{\delta} \bar{u}\, d\bar{z} \tag{9}$$

For the Reynolds numbers of interest here, the Ekman layer flow is expected to be laminar; for such cases the flux integral on the right has previously been represented approximately as one or the other of the following

$$\frac{\int_0^{\delta} \bar{u}\, d\bar{z}}{\bar{r}\,(\nu\Omega)^{1/2}} = f(\omega) = \begin{cases} 0.443\,(1-\omega) & \text{(10a)} \\ \frac{1}{2}\sum_{n=0}^{7} a_n \omega^n & \text{(10b)} \end{cases}$$

The upper, linear expression in Eq. (10a) was used by Wedemeyer.[10] The series given in Eq. (10b) is a polynominal fit by Goller and Ranov[24] to the more refined numerical

data of Rogers and Lance.[26] An analogous expression for this flux has also been derived for situations where the Ekman layer flow is expected to be turbulent.[10] Substituting Eq. (10) into (9) gives, in dimensionless form,

$$u_{BEL} = -Re^{-1/2} \frac{R}{H} \frac{r}{\bar{Z}_{FS}} f(\omega) \tag{11}$$

As for the free surface motion, the flux across any radial surface, $\bar{r}$, should equal the rate of change of fluid volume between the axis and $\bar{r}$. Again, this is spread uniformly over the height of the fluid column:

$$2\pi \bar{r}\, \bar{Z}_{FS}\, \bar{u}_{FS} = -2\pi \int_0^{\bar{r}} \frac{\partial \bar{Z}_{FS}}{\partial \bar{t}}\, \bar{r}'\, d\bar{r}'$$

or in dimensionless form,

$$u_{FS} = -\int_0^r \frac{\partial Z_{FS}}{\partial t}\, r'\, dr' \Big/ (r\, Z_{FS}) \tag{12}$$

where backward differencing is used for $\partial Z_{FS}/\partial t$,

$$\left.\frac{\partial Z_{FS}}{\partial t}\right)_i^{i+1} = \frac{Z_{FS_i}^{i+1} - Z_{FS_i}^{i}}{\Delta t} + O(\Delta t) \tag{13}$$

and Simpson's rule is again used for the quadrature. Use of Eqs. (11) - (13) in (7) completes the evaluation of u in terms of v needed in Eq. (3b). The above analysis of Stage 1 conditions is identical to that used by Goller and Ranov, except for the use of an implicit, as opposed to their explicit, time-marching scheme.

It is shown in Appendix A that for $F > 4(1 - L/H)$ the flow will at some time intersect the top endwall. This will be evidenced by Eq. (8a) predicting $Z_1 > 1$. The flow is now in Stage 2b, which is discussed next.

---

26. Rogers, M.H., and Lance, G.N., "The Rotationally Symmetric Flow of a Viscous Fluid in the Presence of an Infinite Rotating Disk", J. of Fluid Mechanics, Vol. 7 Pt. 4, 617-631, 1960.

Stage 2b

Suppose that the point at which the integral in Eq. (8a) first exceeds (1 - L/H) lies in the interval between grid points $r_j = r_L$ and $r_{j+1} = r_R$, i.e., $r_L \le r_H \le r_R$. Using linear interpolation, the integrand is expressible as

$$g(r) \equiv v^2 r = b + 2a(r - r_L) \qquad r_L \le r \le r_R \tag{14}$$

where

$$b = g_L$$

$$a = (g_R - g_L) / (2\Delta r)$$

If Eq. (14) is substituted into Eq. (8a), and Z_1 is set to unity, the following quadratic is obtained for r_H:

$$aF(r_H - r_L)^2 + bF(r_H - r_L) + FI_L - (1 - L/H) = 0$$

where $I_L = \int_0^{r_L} g(r)\,dr$. The appropriate root ($r_H > r_L$) is

$$r_H = r_L + \frac{-bF + \left\{(bF)^2 - 4(aF)\left[FI_L - (1 - L/H)\right]\right\}^{1/2}}{2aF} \tag{15}$$

This represents the radius of intersection with the top endwall. For $r \ge r_H$, $Z_{FS} = 1$ (see Figure 1) while for $r < r_H$ Eq. (A-11) is used,

$$Z_{FS}(r,t) = 1 - F\int_r^{r_H} \frac{v^2}{r'}\,dr' \tag{16}$$

integrating in towards the axis, r = 0.

Applying the same arguments as in Stage 1, we find for u_{FS}

$$u_{FS} = -\int_0^r \frac{\partial Z_{FS}}{\partial t}\, r'\,dr' \Big/ (r Z_{FS}) \qquad 0 \le r \le r_H \tag{17a}$$

$$u_{FS} = 0 \qquad r_H \le r \le 1 \tag{17b}$$

One can show from continuity arguments that the integral in Eq. (17a) vanishes at $r = r_H$, and hence u_{FS} remains continuous there.

Next consider the Ekman layer pumping. The contribution from the bottom wall is the same as in Stage 1,

$$u_{BEL} = -Re^{-1/2} \frac{R}{H} \frac{r}{Z_{FS}} f(\omega) \tag{18}$$

But the top wall is only partially wetted. The author is unaware of any published investigations into the nature of the boundary layer that forms in such a case. At the very least, one expects that the outward flux in the layer must vanish at r_H, since there is no longer any fluid at $r < r_H$ to sustain it. So to the mass flux in Eq. (10), and hence u_{TEL}, is added a pre-multiplicative factor, $K_T (r - r_H)^{\gamma_T}$, to reflect this:

$$u_{TEL} = 0 \qquad 0 \le r \le r_H \tag{19a}$$

$$u_{TEL} = -Re^{-1/2} \frac{R}{H} r K_T (r - r_H)^{\gamma_T} f(\omega) \qquad r_H \le r \le 1 \tag{19b}$$

where K_T, $\gamma_T > 0$.

Such a heuristic extension of the arguments put forth by Wedemeyer and Goller and Ranov satisfies the following constraints:

- u remains continuous across $r = r_H$;
- the contribution from u_{TEL} vanishes at both $r = r_H$ and 1, as it should;
- the influence of the top endwall Ekman layer will increase as r_H decreases, which is intuitively satisfying;
- the columnar nature of the flow is maintained.

Certainly other analytical forms can be found which would satisfy these constraints. But in the absence of any experimental data to serve as a guide, it was decided to employ the simplest form possible. For the calculations reported here, K_T and γ_T were both set to unity.

Eq. (A-28) indicates that for $F > (1 - L/H)^{-1}$ eventually the fluid displacement will expose a portion of the bottom endwall. This will be indicated during the evaluation of Eq. (16) if at some r, Z_{FS} becomes negative. The flow is now in its final configuration, Stage 3.

Stage 3

Once the bottom endwall is intersected, one cannot expect the boundary condition in Eq. (4a) to apply, as there is no longer any fluid at the axis. Instead, since the fluid depth goes to zero at the intersection point, r_o, it seems appropriate to impose a no-slip boundary condition there,

$$v(r_o) = r_o \tag{20}$$

and to include only those grid points $r_j > r_o$ in the solution of Eq. (3). These changes can be handled with a straightforward modification to the solution algorithm used in Stages 1 and 2b (see Appendix B).

A description of the free surface contour as $z = Z_{FS}(r, t)$ can be developed for this stage just as was done in the earlier stages. But such a development suffers from two significant disadvantages. Whereas during Stage 2b we had only one time-varying limit of integration, r_H, during Stage 3 we have the added complication of r_o also changing with time. Moreover, it is not possible to represent either of these limits explicitly in terms of the given velocity profile. Secondly, the free surface in this stage is typically quite steep, so that the accuracy of the numerical quadratures on the radial grid comes into question.

Both obstacles may be overcome by turning our frame of reference sideways. That is, we can just as well choose z as our independent variable and let $r = R_{FS}(z, t)$ represent the surface contour (see Figure 1). In this frame the fluid is always constrained between the constant limits z = 0 and 1. More important, the surface has a shallow slope, allowing the application of standard quadrature techniques. From Eqs. (A-22) and (A-24), the free surface will now evolve according to

$$r_o^2(t) = 1 - \frac{L}{H} - \frac{2}{F}\int_0^1 \frac{R_{FS}^2(z,t)(1-z)\,dz}{v^2(z,t)} \tag{21a}$$

$$R_{FS}^2(r,t) = r_o^2(t) + \frac{2}{F}\int_o^z \frac{R_{FS}^2(z',t)\,dz'}{v^2(z',t)} \qquad (21b)$$

where v(z, t) is understood to mean $v(R_{FS}(z, t), t)$. This defines the contour implicitly. For a given v(r, t), Eq. (21) may be viewed as an integral equation for R_{FS}^2. It is also weakly nonlinear owing to the implicit dependence of v(z, t) on the solution. As a result, during Stage 3, in addition to the "outer" iteration on v used to solve Eq. (3), we will now have an "inner" iteration process to determine the free surface contour consistent with v.

To solve Eq. (21), a uniform grid is laid out in the z direction, $z_k = (k - 1)\,\Delta z$, $k = 1,2 \ldots NK$ where $\Delta z = 1/(NK - 1)$. On the initial transition to Stage 3, a first guess at R_{FS} is made by fitting a cubic spline[27] through the ordered pairs (Z_{FS_j}, r_j) obtained from Eq. (16). This spline is then evaluated at all the z_k, which specifies $R_{FS_k} = R_{FS}(z_k, t)$. On succeeding steps in Stage 3, the first guess to R_{FS} is taken to be that from the previous time step. Next, a cubic spline is passed through the point (r_o, r_o) (see Eq. (20)) and the ordered pairs (r_j, v_j); again only those $r_j > r_o$ are included in the fit. This spline is then evaluated at all the R_{FS_k}, which defines $v_k = v(z_k, t)$.

Having thus specified $R_{FS}(z, t)$ and a self-consistent v(z, t) in discrete form, the quadratures in Eq. (21) are performed using Simpson's rule. Convergence is achieved when this solution agrees, at each k, with the previous estimate to within some prescribed relative error. If not, the solution is relaxed according to

$$R_{FS}^{(n+1)} = \beta R_{FS}^{s} + (1 - \beta) R_{FS}^{(n)} \qquad (22)$$

where $R_{FS}^{(n)}$ represents the nth iterate, and R_{FS}^{s} represents the solution vector to Eq. (21) based on this iterate. Note that to remain self-consistent the velocity spline defining v_k must be refit and reevaluated at each iteration. For linear equations, it can be shown (e.g., Reference 28) that $\beta = 1$ will yield converged solutions. In our case, the nonlinearity necessitated underrelaxing the iterations; a value of $\beta = 0.5$ was used and typically no more than 4-5 iterations were required for convergence. When a solution is reached, cubic splines are again employed to revert from $R_{FS}(z_k, t)$ back to $Z_{FS}(r_j, t)$.

---

27. IMSL Library Reference Manual, 8th Ed., Vol. 1, Chapter I, IMSL Inc., Houston, Texas, 1980.
28. Hildebrand, F.B., Methods of Applied Mathematics, 2nd. Ed., Chapter 3, Prentice-Hall, Inc., Englewood Cliffs, N.J., 1965.

Using the same physical arguments as in the earlier stages, but with r replaced by z as the integration variable, leads to the following equation for u_{FS}:

$$u_{FS} = \int_0^{z_{FS}} R_{FS} \frac{\partial R_{FS}}{\partial t} \, dz' \Big/ (r z_{FS}) \qquad r_o \le r \le r_H \qquad (23a)$$

$$u_{FS} = 0 \qquad r_H \le r \le 1 \qquad (23b)$$

where, analogous to Eq. (13),

$$\left.\frac{\partial R_{FS}}{\partial t}\right)_k^{i+1} = \frac{R_{FS_K}^{i+1} - R_{FS_K}^{i}}{\Delta t} + O(\Delta t) \qquad (24)$$

It is clear that u_{FS} vanishes at $r = r_o$ ($Z_{FS} = 0$); one can also show from conservation of fluid volume that $u_{FS} = 0$ at $r = r_H$ ($Z_{FS} = 1$), as it should. In evaluating Eq. (23), first Simpson's rule is used to perform the integration with the upper limit replaced by z_k, for all k = 1,2 . . . NK. A cubic spline is then fit through these flux integrals, effectively defining the flux as a continuous function of z. The value of this spline at Z_{FS_j} then represents the numerator in Eq. (23) needed to obtain u_{FS_j}. It should be emphasized here that the axial grid is used only to evaluate Eqs. (21) and (23) pertaining to the free surface motion. Eq. (3) for the azimuthal velocity is still solved on the radial grid.

The radial velocity contribution from the top Ekman layer is still given by Eq. (19). The contribution from the bottom layer is now also presumed reduced by a pre-multiplicative factor to reflect the fact that it no longer covers the entire wall:

$$u_{BEL} = 0 \qquad r \le r_o \qquad (25a)$$

$$u_{BEL} = -Re^{-1/2} \frac{R}{H} \frac{r}{z_{FS}} K_B \left(1 - \frac{r_o}{r}\right)^{\gamma_B} f(\omega) \qquad r_o \le r \le 1 \qquad (25b)$$

where K_B, $\gamma_B > 0$; both were set to unity for the calculations presented here. This expression satisfies our intuitive expectations that u_{BEL} should vanish at r_o, and that its contribution at any r should grow progressively smaller as more of the wall is exposed.

In closing this section, we wish to recognize that the model described above, heuristic as it is, forms a rather simplified picture of a complex flowfield. But the equations are felt to adequately describe the gross features of the phenomena, and as such should provide a useful first step towards a deeper understanding. We are buoyed in this belief by the successful correlations with experiment of the earlier simplified models of Wedemeyer[10] and Goller and Ranov.[24]

Section 3
NUMERICAL RESULTS AND DISCUSSION

To uniquely define the problem, one must specify values for Re, F, H/R and L/H. Values of these input parameters for the cases to be discussed here are summarized in Table 1, along with the temporal and radial grid sizes used. Representative calculations were made for smaller values of Δr and Δt to insure that convergence had been achieved. The cases include flows whose final configurations lie in each of the three permissible stages. For those cases where Stage 3 was achieved NK = 51 axial grid points were used for the free surface integrations. In all cases Eq. (10b) was used to represent the nominal Ekman layer flux. A relative error criterion of 10^{-3} was used for both the velocity iterations, and the free surface iterations during Stage 3.

Table 1
INPUT PARAMETERS FOR CASES 1-6

Case No.	Re	F	H/R	L/H	Final Configuration	Δt	Δr
1	2.293×10^5	0.6746	2.865	0.8	Stage 1	9.251	0.02
2	1.172×10^5	4.141	3.0	0.8	Stage 2b	5.0	0.02
3	1.172×10^5	3.5	3.0	0.6	Stage 3	5.0	0.02
4	1.172×10^4	3.5	3.0	0.6	Stage 3	2.0	0.02
5	1.172×10^3	3.5	3.0	0.6	Stage 3	0.5	0.02
6	1.172×10^5	6.0	3.0	0.8	Stage 3	5.0	0.01

A problem occurs in defining when the fluid is fully spun up which is similar to that which arises in defining the "edge" of a boundary layer - the condition is approached only asymptotically. As shown in Appendix A, the final fluid configuration, and corresponding angular momentum, depend only on L/H and F. Hence the latter can be computed a priori. At each step in the calculation, the current angular momentum is evaluated and referenced to this final value. The instant at which this ratio first equals or exceeds 0.99 will be used here as the definition of the spin-up time, t_S.

The conditions for Case 1 were chosen to match those given in Figures 10 and 14 of Reference 24, which include experimental data. As noted earlier, for such Stage 1 flows the present model is virtually identical to Goller and Ranov's, save for the use here of an implicit algorithm. The odd time increment in Table 1 was chosen as a convenient sub-multiple of the dimensional time increments at which experimental data were taken. The predicted azimuthal velocity profiles and free surface contours are shown in Figures 2a and 2b, respectively, at selected instants of time. Note in Figure 2b that the axial coordinate has been renormalized to the same scale as the radius to better reflect the true picture. The dots represent data read from Goller and Ranov's curves for $\bar{t} = 100$ and 400 sec.; the agreement with the present calculations is quite good. No experimental data were taken for the velocity profiles. The theory predicts that solid-body rotation is achieved at $\bar{t}_S = 570$ sec., the last instant shown.

The conditions for Case 2 were chosen so that the final fluid configuration would be in Stage 2b. Velocity and free surface profiles for this case are shown in Figure 3 for dimensionless times out to $t_S = 4000$ in increments of 400. The upper endwall is intersected early on in the calculation, at $t = 200$. The asymptotic approach to solid-body rotation is clearly evident in the bunching up of the curves toward the end of the calculation. Unfortunately, no quantitative experimental data are available for flows in Stage 2b.

For the linearized spin-up of fluid without a free surface, the basic time dependence has been shown to be exponential.[8] The question was raised in the published discussion following Reference 24 of whether similar behavior would be found for cases such as those studied here, where nonlinear convective terms are retained and a free surface is present. If such is the case, one might expect the fluid angular momentum to evolve according to

$$\frac{L_z(t)}{L_z(\infty)} = 1 - e^{-at/Re^{1/2}} \tag{26}$$

where "a" is a dimensionless constant. The denominator of the exponential is suggested by the finding that for linearized flows, t_S scales with $Re^{1/2}$ (Reference 8). If the present calculations do indeed reflect such behavior, then a semi-logarithmic plot of the momentum deficit, $1-L_z(t)L_z(\infty)$, vs. $Re^{-1/2}$ t should yield a straight line. Such a plot is presented in Figure 4 for Cases 1 and 2. The symbols represent numerical data from the present program; a straight line has been faired through the data for each

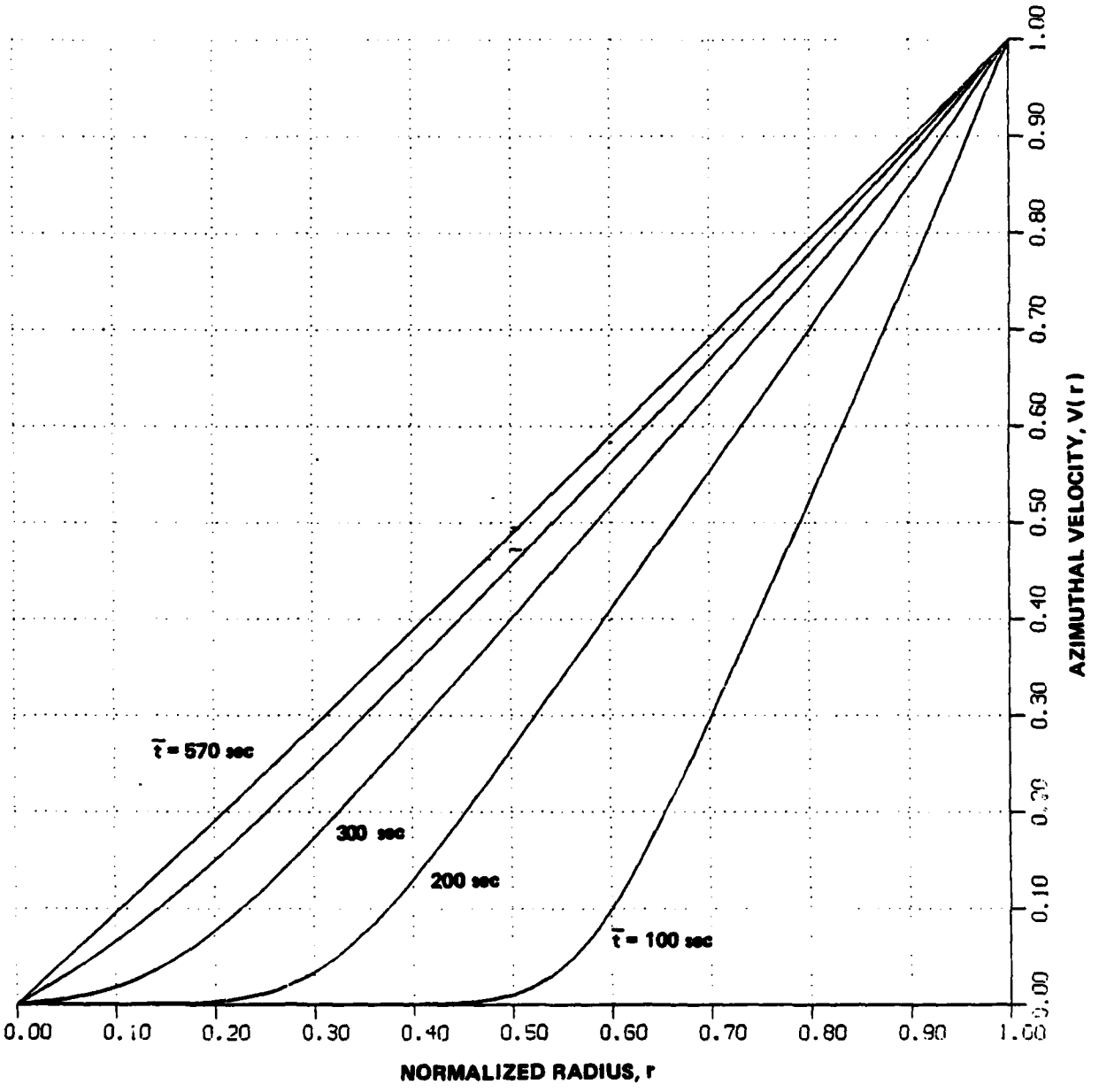

Figure 2a AZIMUTHAL VELOCITY PROFILES FOR CASE 1

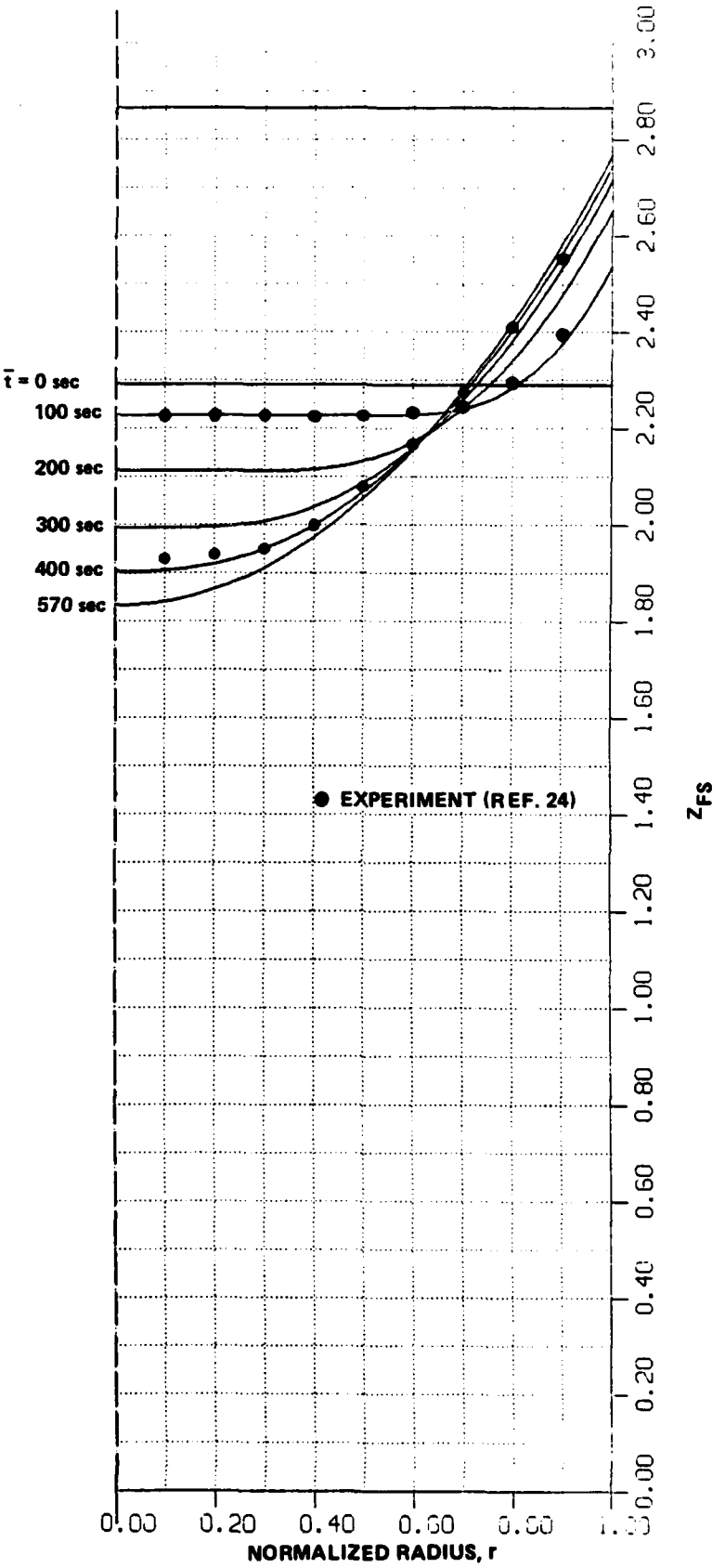

Figure 2b FREE SURFACE CONTOURS FOR CASE 1

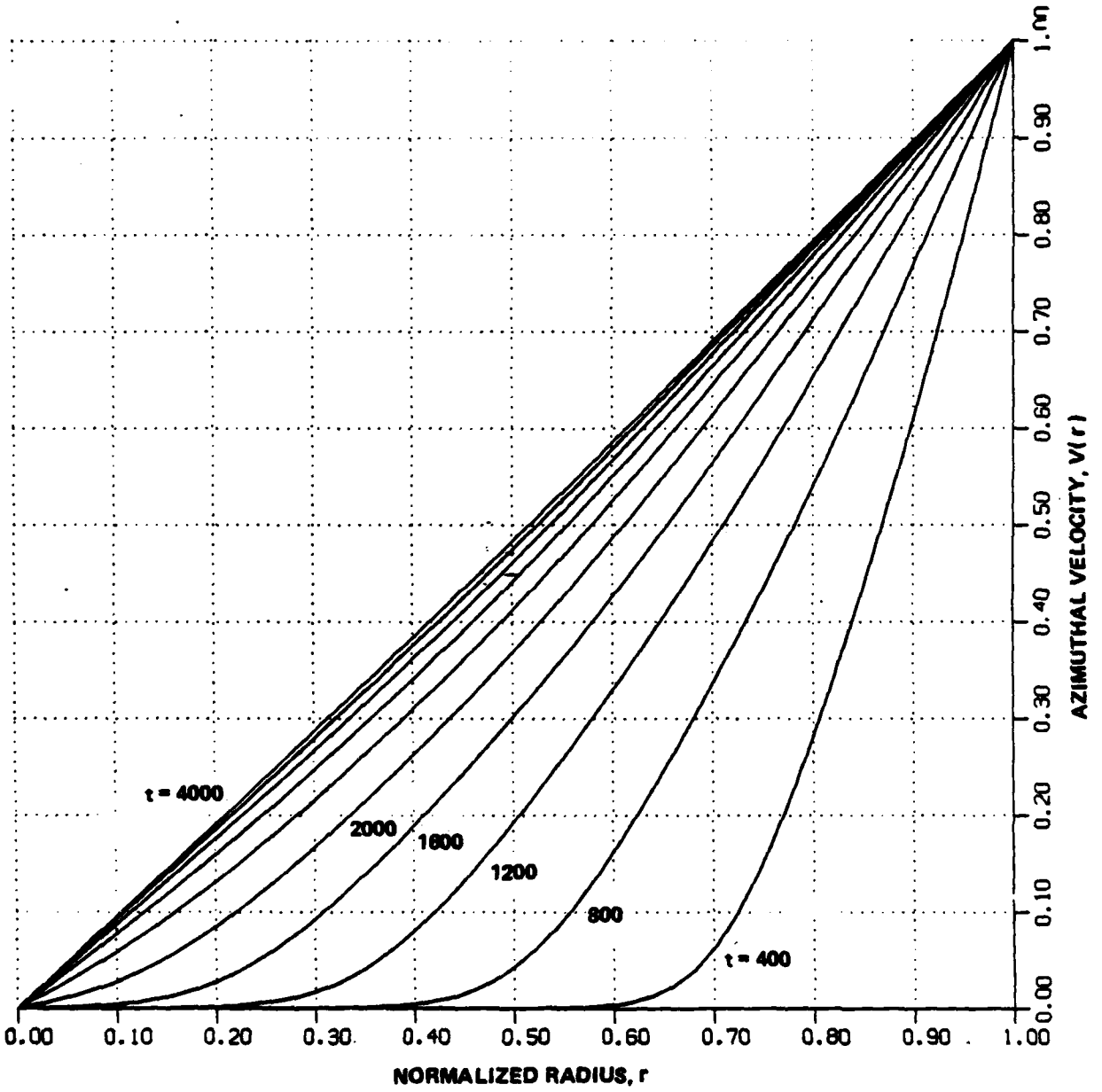

Figure 3a AZIMUTHAL VELOCITY PROFILES FOR CASE 2

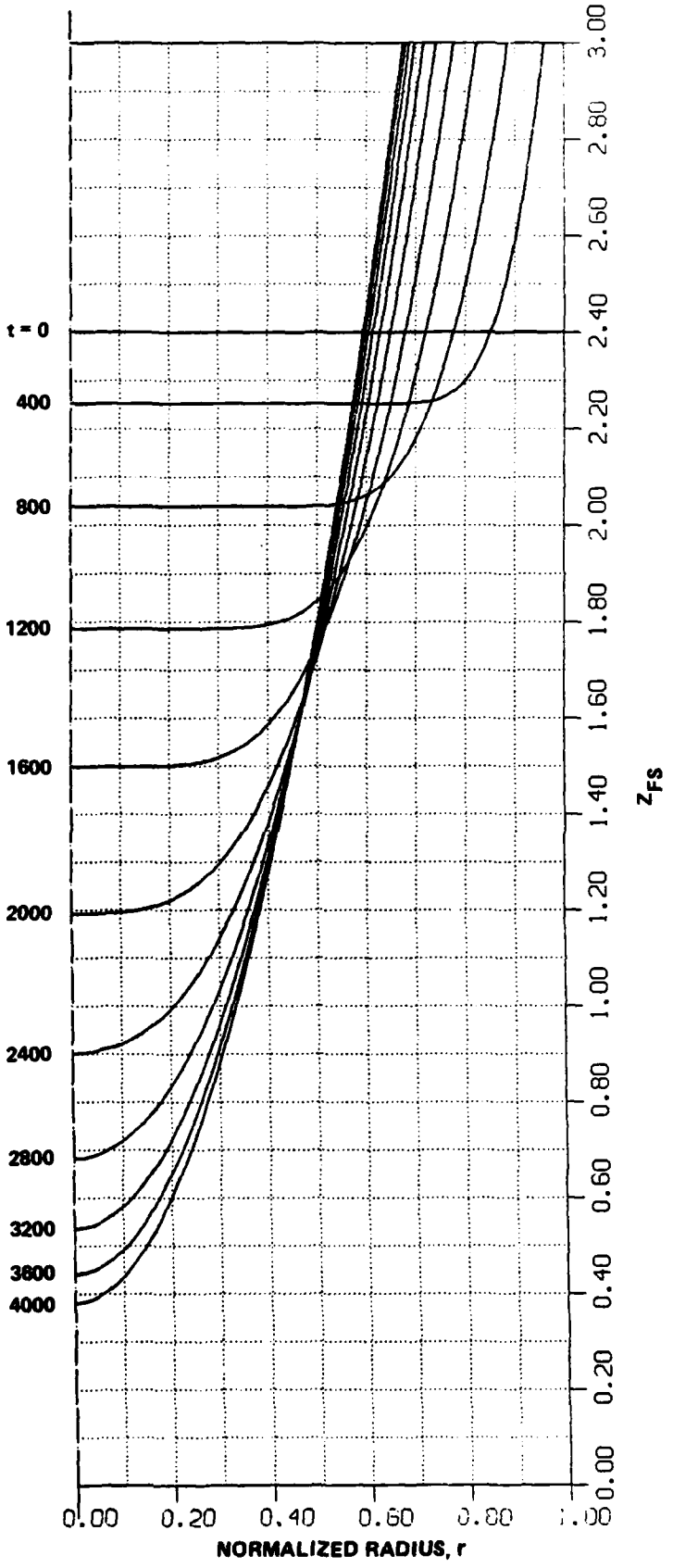

Figure 3b FREE SURFACE CONTOURS FOR CASE 2

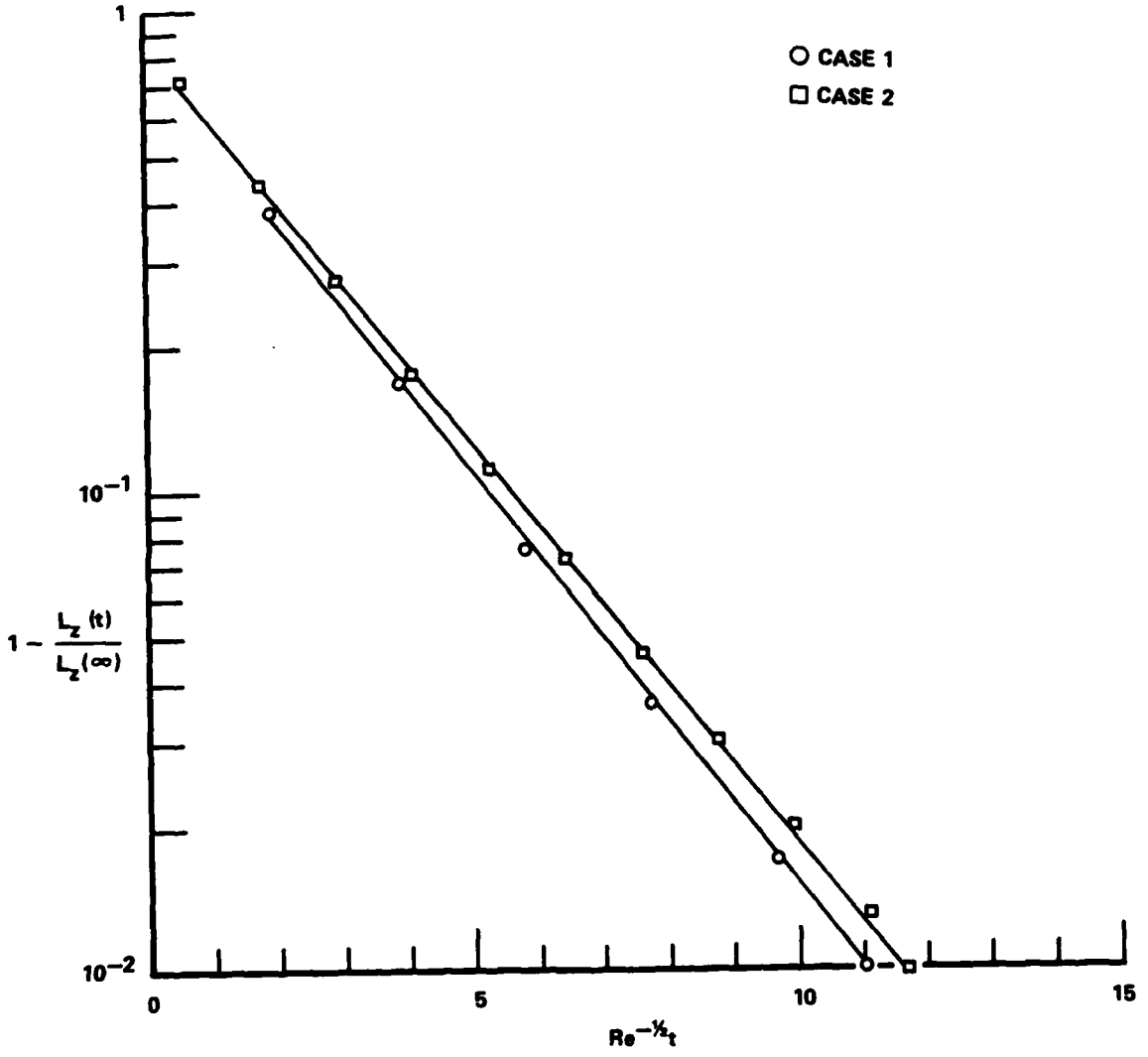

Figure 4 ANGULAR MOMENTUM DEFICIT VS. TIME FOR CASES 1 AND 2

case. It is somewhat remarkable to see the degree to which the data do in fact adhere to a pure exponential behavior. Evidently, however, the $Re^{1/2}$ time scaling is not perfect, as the two cases fail to collapse to a single line; also, F and H/R were different in the two calculations.

Cases 3 through 5 are for conditions such that the final fluid configuration is in Stage 3. They differ only in the values specified for Re, which range over two orders of magnitude. Figure 5 shows the velocity and free surface profiles for Case 3; results for the other two are qualitatively similar. The first nine curves in Figure 5a represent v(r) at dimensionless times t = 400 through 3600 in increments of 400. The last curve is at t_S = 4590; Cases 4 and 5 produced values of t_S = 1200 and 231, respectively. The last five curves end abruptly at $r = r_o$ because there is no fluid to the left of this point, and so v is undefined there.

The free surface profiles in Figure 5b are given for the same times. Again the asymptotic nature of the approach to solid-body rotation is evident in both figures. It is also clear that the surface contours become quite steep, and thus warrant the extra effort spent in Stage 3 in switching from a radial to an axial grid for the surface integrals. Again, no experimental data for flows in this stage are available for comparison.

An anomaly was noted in the radial velocity distribution during Stage 3 of Cases 3-5. Ordinarily u(r), as predicted by Eqs. (7), (19), (23) and (25), is negative, i.e., there is a net inward flux in the core flow. However, for some inboard radii it was noted that u became positive. Such a sign change is inconsistent with a columnar flow model in the absence of sources or sinks. However, rather than representing any fundamental flaw in the numerical algorithm, such behavior merely reflects our inadequate knowledge of the magnitude of the Ekman pumping embodied in Eqs. (19) and (25). Indeed, in the absence of quantitative data for such flows, it is difficult to assess the degree to which the columnar flow approximation remains valid in the vicinity of the intersection point r_o. To keep this from further influencing the solution, at such points u was set to zero. Since by this time the fluid had acquired in excess of 90% of its final momentum, it is doubtful that this would have a serious effect on the results.

The momentum deficit vs. time for Cases 3-5 is shown in Figure 6. Two flagged symbols are shown for each case; these represent the instants just after the transition

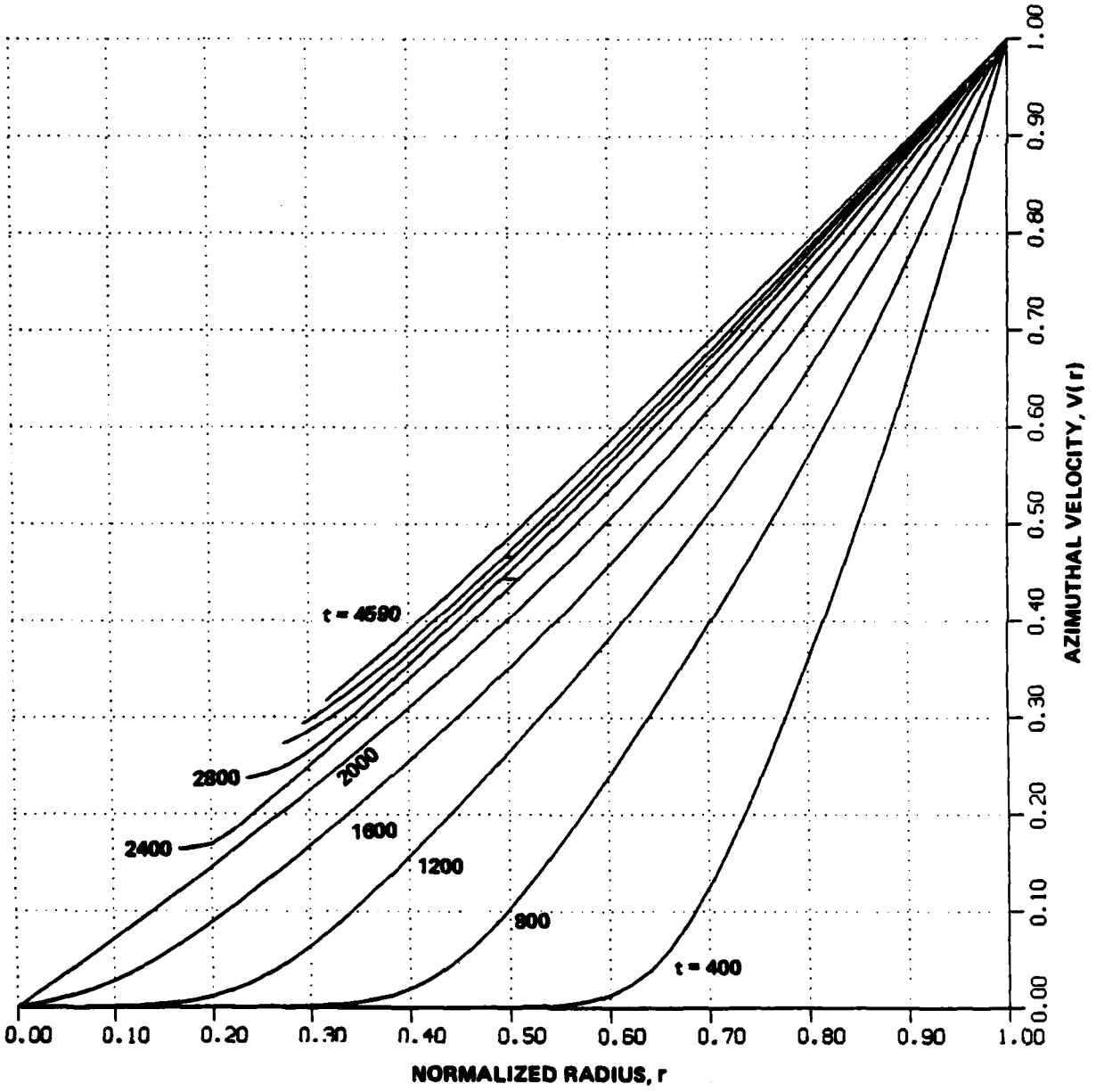

Figure 5a AZIMUTHAL VELOCITY PROFILES FOR CASE 3

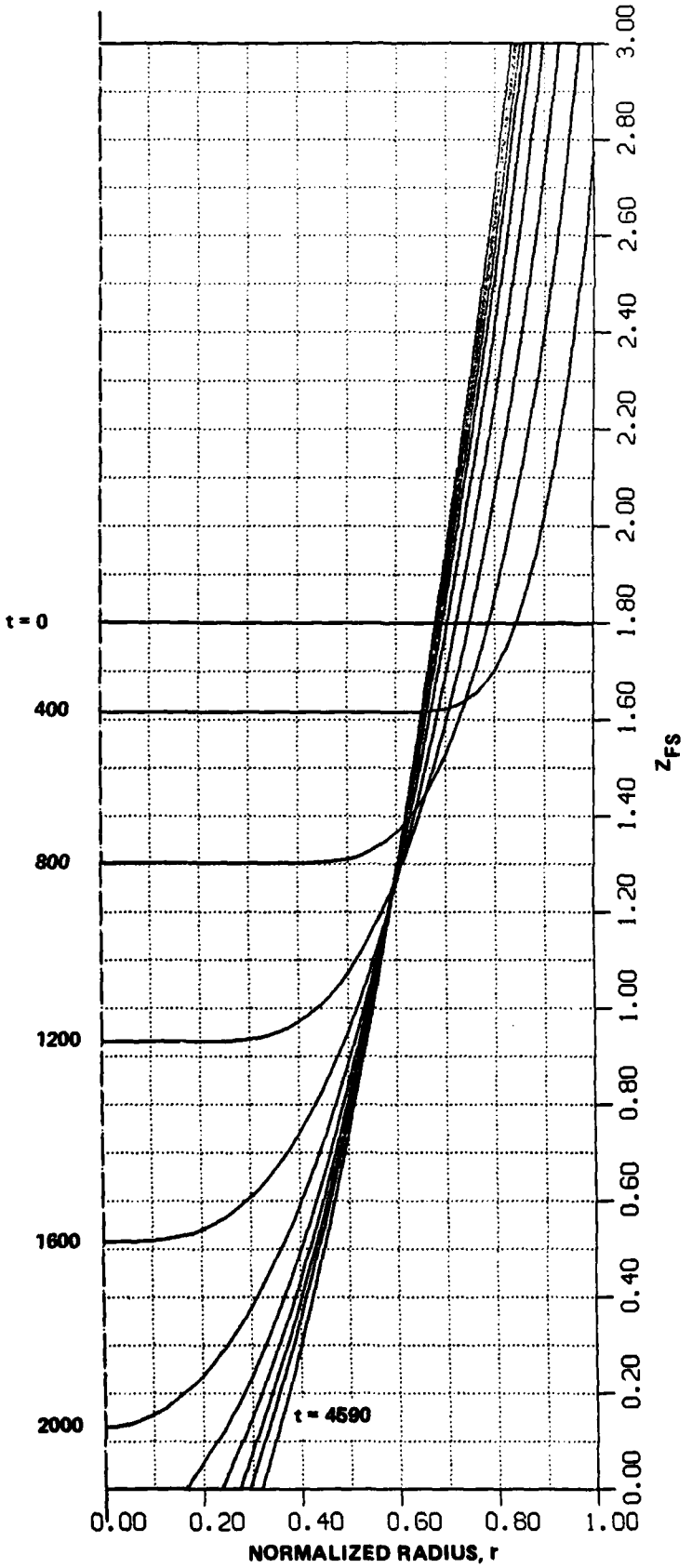

Figure 5b FREE SURFACE CONTOURS FOR CASE 3

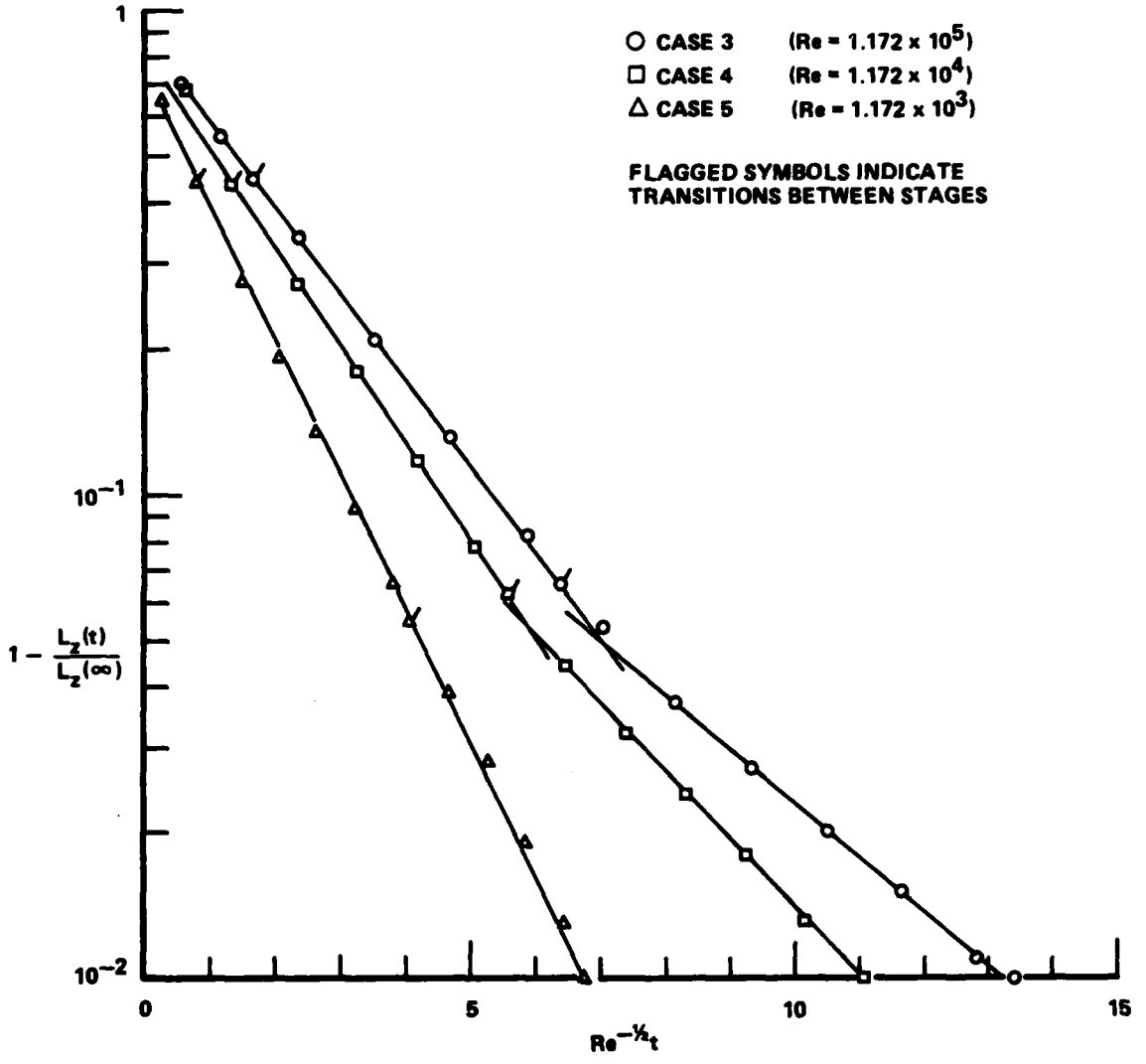

Figure 6 ANGULAR MOMENTUM DEFICIT VS. TIME FOR CASES 3 THRU 5

between stages. Note that the numerical data for Cases 3 and 4 each follow a line of constant slope during the first two stages, as was the case in Figure 4. After the transition to Stage 3, however, the results follow a line with a reduced slope, indicating a slower rate of spin-up. The fact that the first transition apparently has little effect on the rate of spin-up can be explained by noting that the radial extent of the fluid layer at the top wall in Figure 5b is relatively thin. Hence its contribution to the Ekman pumping remains small compared with that from the bottom layer, which still completely covers the wall. Upon making the transition to Stage 3, however, the strength of the bottom Ekman layer pumping is progressively reduced as the wall is exposed, and a slower spin-up rate results.

The results for Case 5, the lowest Re, would seem to represent an exception to the rule. All the numerical data for this case appear to follow a single straight line, with no kink at the second transition. The following qualitative argument is offered to explain this behavior. The Reynolds number, broadly speaking, represents the ratio of convective to viscous forces. For Cases 3 and 4 Re was large enough for the convective, i.e., secondary flow, effects to dominate. Since the secondary flow is driven by the endwall Ekman layers, it is not surprising that the spin-up rate should depend on which stage the flow is in. For Case 5, however, Re takes on its smallest value, and evidently viscous diffusion from the sidewall plays a greater role. Clearly, for this mechanism the degree to which the endwalls are exposed is not as critical, and consequently the spin-up rate is more uniform. Finally, it is interesting to note in Figure 6 that the angular momentum ratios at the times at which transitions occur are nearly independent of Re.

Case 6 is similar to Case 3 except that the values of both L/H and F have been raised. The velocity and free surface profiles for this case are shown in Figure 7. The first nine curves represent t = 400 through 3600 in increments of 400, while the last is at t_S = 4060. As expected, the higher Froude number in this case results in a steeper surface contour than was exhibited for Case 3. The momentum deficit vs. time is plotted in Figure 8, where the data for Case 3 have also been repeated for comparison. During the first two stages, both cases collapse to nearly the same straight line. Note, however, that in Case 6 the free surface intersects the top wall much sooner, and the bottom wall much later, reflecting the higher fill ratio. A discontinuity in slope is again exhibited at the second transition.

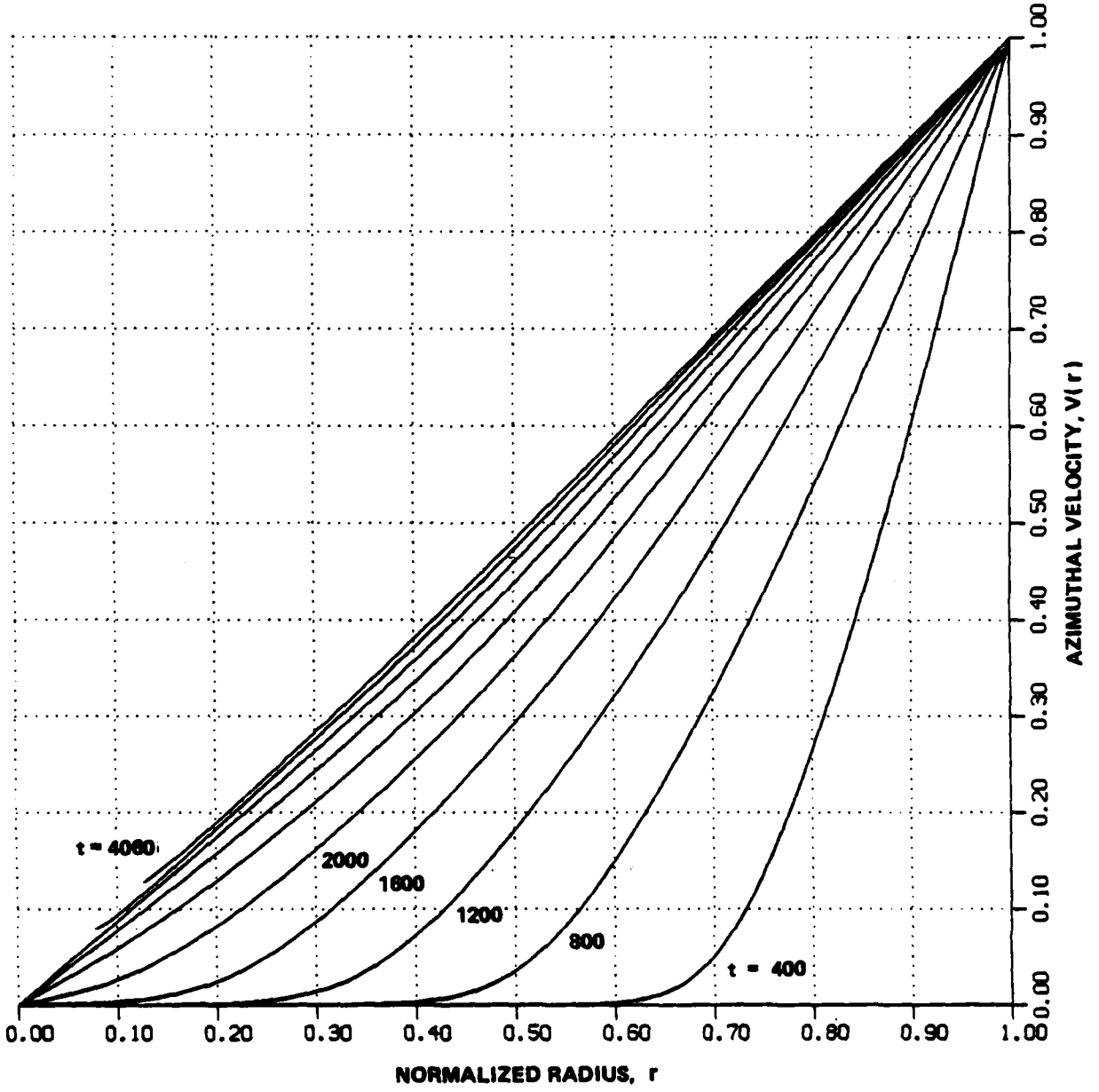

Figure 7a AZIMUTHAL VELOCITY PROFILES FOR CASE 6

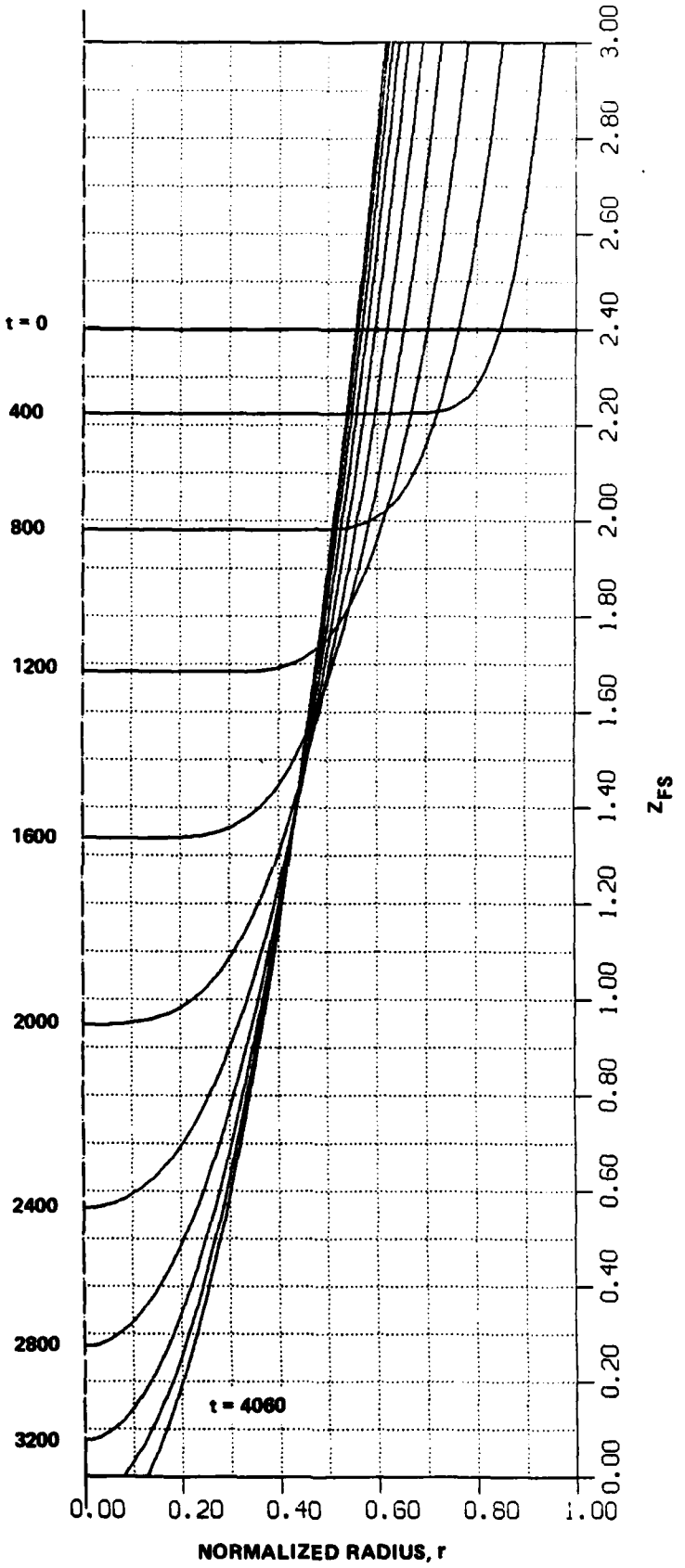

Figure 7b FREE SURFACE CONTOURS FOR CASE 6

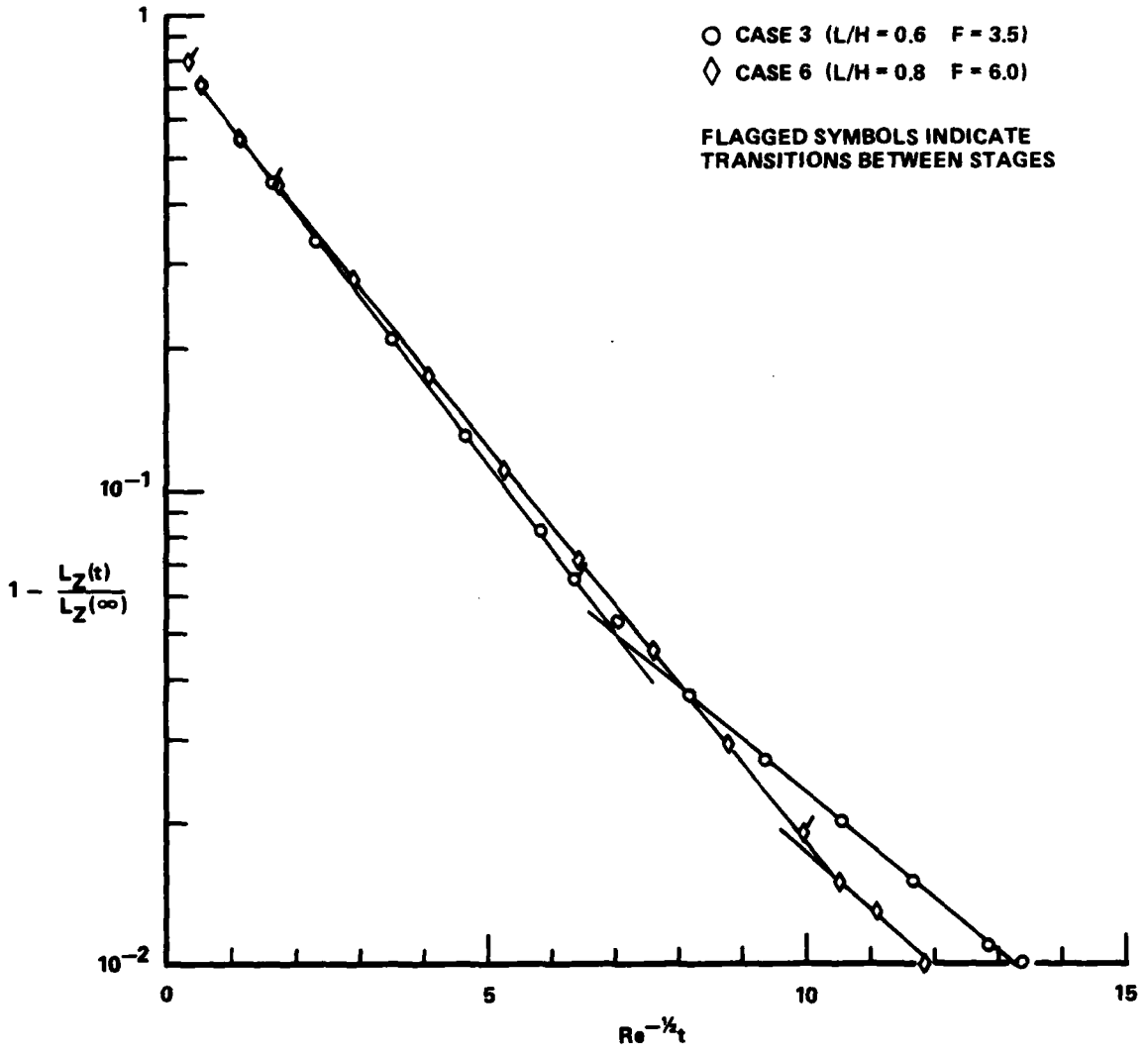

Figure 8 ANGULAR MOMENTUM DEFICIT VS. TIME FOR CASES 3 AND 6

The run times for these calculations varied from 0.73 min. for Case 1 to 3.3 mins. for Case 6, using an IBM 370/3031 system. But such numbers are to a certain extent arbitrary, depending as they do on what temporal and spatial grid sizes were used. A more meaningful measure is the CPU time per time step per grid point. This was approximately 1.5×10^{-3} sec. for the first two cases, and about double that value for the remainder. The latter no doubt took longer because of the additional iterations needed to define the free surface.

Section 4
SUMMARY AND CONCLUSIONS

A theoretical analysis is presented for the axisymmetric spin-up of fluid in a partially-filled cylindrical cavity. The analysis represents an extension of the earlier treatments by Wedemeyer,[10] and Goller and Ranov,[24] to those cases where the liquid free surface may intersect one or both endwalls. Earlier estimates of the Ekman layer pumping of the secondary flow are modified heuristically for situations where the layer no longer covers the entire wall. Also, due to the very steep free surface contour in the latter stages of spin-up, it was found advantageous to develop the free surface equations in an axial, rather than radial, coordinate frame.

A computer program has been developed which solves the governing nonlinear equations using a straightforward finite-difference algorithm. The code predicts both the azimuthal velocity distribution with radius, and the free surface contour, as functions of time. Predictions for the latter agree with Gerber's[22] steady-state analysis as the limit of solid-body rotation is approached. The present results also exhibit very good agreement with the time-resolved experimental data for the surface contour taken by Goller and Ranov.[24] Their data were taken only for situations where the free surface did not touch the endwalls. At present, there are no quantitative data against which the present analysis can be compared for cases where one or both endwalls are intersected.

Nevertheless, the following qualitative conclusions have been drawn from the theory. Plotting the fluid angular momentum deficit vs. $Re^{1/2}$ t appears to correlate the numerical data reasonably well, although the collapse is by no means perfect. Such plots indicate that the angular momentum transfer follows a simple exponential behavior in time. For Re in the range 10^4 - 10^5, the growth rate appears uniform up to the point where the bottom endwall is intersected. After this, exponential behavior is still exhibited, but at a reduced rate, reflecting the diminishing influence of the bottom Ekman layer which is primarily responsible for the secondary flow. For Re on the order of 10^3, a uniform growth in momentum is exhibited over the whole of the calculation, perhaps suggesting that such flows are dominated by viscous diffusion from the sidewall.

To validate the analysis in a quantitative sense, it is recommended that its predictions be compared with suitably designed laboratory experiments and/or more

refined numerical calculations, e.g., solutions of the full axisymmetric Navier-Stokes equations. Such comparisons could also serve as guidelines for adjusting the empirical parameters in Eqs. (19) and (25) used to define the strength of the Ekman pumping. It is felt that the present computer code could then serve as an efficient means of predicting fluid spin-up in cases of practical interest. Such predictions form an integral part of any attempt to predict the spin-decay of liquid filled projectiles,[3,4] and the eigenfrequencies of the perturbed fluid motion,[5,6] both of which are of critical importance in determing the projectile's stability.

REFERENCES

1. Engineering Design Handbook. Liquid-Filled Projectile Design, AMC Pamphlet No. 706-165, U.S. Army Materiel Command, Washington, D.C., April 1969.

2. Winch, D.M., An Investigation of the Liquid Level at the Wall of a Spinning Tank, NASA TN D-1536, August 1962.

3. Kitchens, C.W., Jr., Gerber, N. and Sedney, R., "Spin Decay of Liquid-Filled Projectiles", J. of Spacecraft, Vol. 15 No. 6, 348-354, December 1978.

4. Kitchens, C.W., Jr. and Gerber, N., Prediction of Spin Decay of Liquid-Filled Projectiles, BRL Report 1996, Aberdeen Proving Ground, Md., July 1977.

5. Kitchens, C.W., Jr., Gerber, N., and Sedney, R., Oscillations of a Liquid in a Rotating Cylinder: Part I. Solid-Body Rotation, ARBRL-TR-02081, Aberdeen Proving Ground, Md., June 1978.

6. Kitchens, C.W., Jr., Gerber, N., and Sedney, R., Oscillations of a Liquid in a Rotating Cylinder: Part II. Spin-Up, BRL Report (in preparation).

7. McLeod, A.R., "The Unsteady Motion Produced in a Uniformly Rotating Cylinder of Water by a Sudden Change in the Angular Velocity of the Boundary", Philosophical Magazine and Journal of Science, Vol. 44, No. 259, 1-14, 1922.

8. Greenspan, H.P. and Howard, L.N., "On a Time-Dependent Motion of a Rotating Fluid", J. of Fluid Mechanics, Vol. 17 Pt. 3, 385-404, 1963.

9. Greenspan, H.P. and Weinbaum, S., "On Non-Linear Spin-Up of a Rotating Fluid", J. of Mathematics and Physics, Vol. 44, 66-85, 1965.

10. Wedemeyer, E.H., "The Unsteady Flow Within a Spinning Cylinder", J. of Fluid Mechanics, Vol. 20 Pt. 3, 383-399, 1964.

11. Benton, E.R., "On the Flow Due to a Rotating Disk", J. of Fluid Mechanics, Vol. 24 Pt. 4, 781-800, 1966.

12. Benton, E.R., "Vorticity Dynamics in Spin-Up from Rest", Physics of Fluids, Vol. 22 No. 7, 1250-1251, 1979.

13. Venezian, G., "Non-Linear Spin-Up", Topics in Ocean Engineering, Vol. 2, 87-96, Gulf Publishing Co., Houston, 1970.

14. Weidman, P.D., "On the Spin-Up and Spin-Down of a Rotating Fluid. Part I: Extending the Wedemeyer Model. Part II: Measurements and Stability", J. of Fluid Mechanics, Vol. 77 Pt. 4, 685-735, 1976.

15. Watkins, W.B. and Hussey, R.G., "Spin-Up from Rest: Limitations of the Wedemeyer Model", Physics of Fluids, Vol. 16 No. 9, 1530-1531, 1973.

16. Watkins, W.B. and Hussey, R.G., "Spin-Up from Rest in a Cylinder", Physics of Fluids, Vol. 20 No. 10, 1596-1604, 1977.

17. Greenspan, H.P., The Theory of Rotating Fluids, Cambridge University Press, London, 1968.

18. Warn-Varnas, A., Fowlis, W.W., Piacsek, S., and Lee, S.M., "Numerical Solutions and Laser-Doppler Measurements of Spin-Up", J. of Fluid Mechanics, Vol. 85 Pt. 4, 609-639, 1978.

19. Kitchens, C.W., Jr., Navier-Stokes Solutions for Spin-Up from Rest in a Cylindrical Container, ARBRL-TR-02193, Aberdeen Proving Ground, Md., September 1979.

20. Kitchens, C.W., Jr., Navier-Stokes Solutions for Spin-Up by a Predictor-Corrector Multiple-Iteration Method, AIAA Paper No. 79-1454, presented at AIAA Computational Fluid Dynamics Conference, July 23-25, 1979, Williamsburg, Va.

21. Mark, A., Measurements of Angular Momentum Transfer in Liquid-Filled Projectiles, ARBRL-TR-2029, Aberdeen Proving Ground, Md., November 1977.

22. Gerber, N., "Properties of Rigidly Rotating Liquids in Closed Partially Filled Cylinders", ASME Transactions, J. of Applied Mechanics, Vol. 97, 734-735, 1975.

23. Gerber, N., Rigidly Rotating Liquids in Closed Partially Filled Cylindrical Cavities, BRL-MR-2462, Aberdeen Proving Ground, Md., March 1975.

24. Goller, H. and Ranov, T., "Unsteady Rotating Flow in a Cylinder with a Free Surface", ASME Transactions, J. of Basic Engineering, Vol. 90D, No. 4, 445-454, December 1968.

25. Richtmeyer, R.D. and Morton, K.W., Difference Methods for Initial Value Problems, 2nd Ed., Chapter 8, Interscience Publishers, New York, 1967.

26. Rogers, M.H., and Lance, G.N., "The Rotationally Symmetric Flow of a Viscous Fluid in the Presence of an Infinite Rotating Disk", J. of Fluid Mechanics, Vol. 7 Pt. 4, 617-631, 1960.

27. IMSL Library Reference Manual, 8th Ed., Vol. 1, Chapter I, IMSL Inc., Houston, Texas, 1980.

28. Hildebrand, F.B., Methods of Applied Mathematics, 2nd. Ed., Chapter 3, Prentice-Hall, Inc., Englewood Cliffs, N.J., 1965.

NOMENCLATURE

F	Froude number, $(\Omega R)^2/gH$
g	axial acceleration (= gravity in a laboratory frame)
H	height of cylinder
i	time index, $t^k = i\,\Delta t$
j	radial grid index, $r_j = (j-1)\,\Delta r$
k	axial grid index, $z_k = (k-1)\,\Delta z$
L	initial fluid level before spin-up
L_z	dimensionless fluid angular momentum about the cylinder's axis, Eq. (A-9)
NJ	number of radial grid points
NK	number of axial grid points used in Stage 3 free surface integrals
p	pressure
$(\bar{r}, \theta, \bar{z})$	dimensional cylindrical coordinates
R	radius of cylinder
r	$\bar{r}/R$
r_o, r_H	dimensionless radii at which endwalls are intersected (Figure 1)
R_{FS}	radial coordinate description of the free surface during Stage 3
Re	Reynolds number, $\Omega R^2/\nu$
t	$\Omega\bar{t}$
t_s	dimensionless spin-up time
(u,v,w)	dimensionless velocities in the (r, θ, z) directions, respectively, normalized by ΩR
u_{TEL}, u_{BEL}	contributions to u from the top and bottom Ekman layers, respectively
u_{FS}	contribution to u from free surface motion
z	$\bar{z}/H$
Z_{FS}	axial coordinate description of the free surface during Stages 1 and 2b
Z_o, Z_l	dimensionless fluid levels at the axis and sidewall, respectively
α	relaxation factor in velocity iterations
β	relaxation factor in free surface iterations
δ	Ekman boundary layer thickness
ν	kinematic viscosity
ρ	density
Ω	angular velocity of cylinder, rad./sec.
ω	dimensionless local angular velocity, $v/r = \bar{\omega}/\Omega$
$(\bar{\ })$	indicates a dimensional variable

Appendix A
FREE SURFACE EQUATIONS

In this appendix we develop the equations used to describe the free surface motion. Following Winch[2] and Goller and Ranov,[24] we assume that surface tension can be neglected, in which case balancing the centrifugal and gravitational body forces acting on a fluid element at the surface yields:

$$\frac{d\bar{z}_{FS}}{d\bar{r}} = \frac{\bar{\omega}^2\bar{r}}{g} = \frac{\bar{v}^2}{g\bar{r}} \tag{A-1}$$

or in dimensionless form (see Nomenclature)

$$\frac{dz_{FS}}{dr} = F\omega^2 r = F\frac{v^2}{r} \tag{A-2}$$

where $z = Z_{FS}(r, t)$ defines the free surface contour. This equation is developed and used differently depending on whether the flow is in Stage 1, 2 or 3 (in Gerber's[22] notation) and each of these is discussed separately below.

Stage 1

This is the case treated by Goller and Ranov, in which neither endwall is intersected. Let $Z_1 = Z_{FS}(1, t)$, i.e., the dimensionless fluid level at the sidewall. Then from (A-2),

$$z_{FS}(r,t) = z_1(t) - F\int_r^1 \frac{v^2}{r'}\,dr' \tag{A-3}$$

Conservation of fluid volume requires that

$$2\pi\int_0^1 z_{FS}\, r\,dr = \pi\frac{L}{H} \tag{A-4}$$

Substituting (A-3) into (A-4) gives

$$2\pi\left\{ z_1\int_0^1 r\,dr - F\int_0^1 r\,dr\int_0^1 \frac{v^2}{r'}\,dr' \right\} = \pi\frac{L}{H}$$

The double integration in the second term can be simplified through an integration by parts with respect to the dummy variable r'.* The result, after rearranging and cancelling common factors, is the following expression for Z_1:

$$Z_1 = \frac{L}{H} + F\int_0^1 v^2 r\,dr \qquad \text{(A-5)}$$

Eqs. (A-3) and (A-5) together define the free surface contour, given v(r, t). For completeness, we note that the on-axis fluid level, $Z_0 = Z_{FS}(0, t)$ can be inferred to be:

$$Z_0 = \frac{L}{H} - F\int_0^1 v^2 \left(\frac{1}{r} - r\right) dr \qquad \text{(A-6)}$$

If the integration by parts noted above is used to simplify Goller and Ranov's Eq. (1c), the result is consistent with (A-6).

In the steady limit of solid-body rotation, v = r, and the integrations in Eqs. (A-5) and (A-6) can be done analytically. One can easily show that

$$\frac{L}{H} = \frac{Z_0(t=\infty) + Z_1(t=\infty)}{2} \qquad \text{(A-7)}$$

From this one can infer under what conditions the flow will remain in Stage 1. For the free surface to first intersect the bottom endwall (Stage 2a) requires that $Z_0 = 0$ and $Z_1 \le 1$, for which (A-6) and (A-7) together imply $L/H \le 1/2$ and $F \ge 4\ L/H$. To intersect the top endwall first (Stage 2b) requires $Z_0 \ge 0$ and $Z_1 = 1$, for which (A-5) and (A-7) together imply $L/H \ge 1/2$ and $F \ge 4\ (1 - L/H)$. For present purposes we are primarily concerned with fill ratios greater than one-half, and so the flow will remain in Stage 1 for all time if

$$F \le 4\left(1 - \frac{L}{H}\right) \qquad \text{(A-8)}$$

As a reference for judging the degree to which the fluid has spun up, we define a dimensionless angular momentum about the axis as

$$L_z(t) = \frac{\bar{L}_z}{2\pi\rho H \Omega R^4} = \int_0^1 Z_{FS}\, v\, r^2\, dr \qquad \text{(A-9)}$$

---

* The author is indebted to Mr. Nathan Gerber for pointing this out.

For flows remaining in Stage 1, in the limit of solid-body rotation, Eqs. (A-3), (A-5), and (A-9) then reduce to

$$L_z(t=\infty) = \frac{1}{4}\left(\frac{L}{H} + \frac{F}{12}\right) \tag{A-10}$$

Stage 2b

We denote by $r_H(t)$ the dimensionless radius at which the top endwall is intersected. To the right of this point, $Z_{FS} = 1$; for smaller radii, we get immediately from Eq. (A-2),

$$Z_{FS}(r,t) = 1 - F\int_r^{r_H} \frac{v^2}{r'}\,dr' \tag{A-11}$$

and

$$Z_o(t) = 1 - F\int_o^{r_H} \frac{v^2}{r}\,dr \tag{A-12}$$

Equation (A-11) *alone is insufficient* to define Z_{FS} given v(r, t), since r_H is also unknown. An additional relation for r_H can be derived as follows. Replace Eq. (A-11) with

$$Z_{FS}(r,t) = Z_o + F\int_o^{r} \frac{v^2}{r'}\,dr' \tag{A-13}$$

and again invoke conservation of fluid volume:

$$2\pi\int_o^{r_H} Z_{FS}\, r\,dr + \pi(1-r_H^2) = \pi\frac{L}{H} \tag{A-14}$$

Substituting from (A-13) one obtains

$$2\pi\left\{Z_o\int_o^{r_H} r\,dr + \int_o^{r_H} r\,dr\int_o^{r}\frac{v^2}{r'}dr'\right\} + \pi(1-r_H^2) = \pi\frac{L}{H}$$

Integrating by parts again simplifies the term containing the double integral, and the result is an alternate expression for Z_o,

$$Z_o(t) = \frac{1}{r_H^2}\left[\frac{L}{H} - (1-r_H^2) - F\int_o^{r_H}\frac{v^2}{r}(r_H^2 - r^2)\,dr\right] \tag{A-15}$$

Equating this to (A-12), several terms cancel, and we are left with

$$F \int_0^{r_H} v^2 r \, dr = 1 - \frac{L}{H} \tag{A-16}$$

As shown in Section 2, this result can be used to infer r_H, and then Eq. (A-11) used for the rest of the contour.

The steady limit of Eq. (A-16) yields

$$r_H (t = \infty) = \left[\frac{4}{F} \left(1 - \frac{L}{H} \right) \right]^{1/4} \tag{A-17}$$

and Eq. (A-12) then becomes

$$Z_o (t = \infty) = 1 - \left[F \left(1 - \frac{L}{H} \right) \right]^{1/2} \tag{A-18}$$

Since $Z_o \geq 0$ for the flow to remain in Stage 2b, we see from Eqs. (A-8) and (A-18) that F must then satisfy

$$4 \left(1 - \frac{L}{H} \right) \leq F \leq \left(1 - \frac{L}{H} \right)^{-1} \tag{A-19}$$

For flows in this stage, the solid-body rotation limit of Eq. (A-9) is found to be

$$L_z (t = \infty) = \frac{1}{4} \left[1 - \frac{4}{3} F^{-1/2} \left(1 - \frac{L}{H} \right)^{3/2} \right] \tag{A-20}$$

Though not treated here, results analogous to these can also be derived for Stage 2a; the steady-state results can be found in Reference 22.

Stage 3

For the reasons discussed in the main text, during this state we choose z as our independent variable and let $r = R_{FS}(z, t)$ describe the free surface contour. Equation (A-2) is rewritten as

$$R_{FS} \, d R_{FS} = \frac{1}{F} \frac{dz}{\omega^2} \tag{A-21}$$

where now it is implicitly understood that $\omega(z, t) = \omega(R_{FS}(z, t), t)$. Defining $r_o(t) = R_{FS}(o, t)$ and integrating (A-21) from the bottom up gives

$$R_{FS}^2(z,t) = r_o^2(t) + \frac{2}{F}\int_o^z \frac{dz'}{\omega^2(z',t)} = r_o^2(t) + \frac{2}{F}\int_o^z \frac{R_{FS}^2(z',t)\,dz'}{v^2(z',t)} \tag{A-22}$$

Conservation of mass requires

$$\int_o^1 R_{FS}^2\,dz = 1 - \frac{L}{H} \tag{A-23}$$

Substituting (A-22) into (A-23),

$$r_o^2 + \frac{2}{F}\int_o^1 dz \int_o^z \frac{dz'}{\omega^2(z',t)} = 1 - \frac{L}{H}$$

The second term can again be reduced to a single integral through an integration by parts. Resetting $\omega = v/r$, the result is

$$r_o^2(t) = 1 - \frac{L}{H} - \frac{2}{F}\int_o^1 \frac{R_{FS}^2(z,t)(1-z)\,dz}{v^2(z,t)} \tag{A-24}$$

where of course $v(z, t)$ is understood to mean $v(R_{FS}(z, t), t)$. Substitution of (A-24) in (A-22) yields

$$r_H^2(t) = 1 - \frac{L}{H} + \frac{2}{F}\int_o^1 \frac{R_{FS}^2(z,t)\,z\,dz}{v^2(z,t)} \tag{A-25}$$

In principle, Eqs. (A-22) and (A-24) define the free surface contour for a given v distribution. But Eq. (A-22) really represents an integral equation for the desired R_{FS}^2, and one which cannot be inverted in closed form. As discussed in Section 2, an iterative relaxation procedure was used to solve it.

The steady limits of Eqs. (A-24) and (A-25) are

$$r_o(t=\infty) = \left[1 - \frac{L}{H} - \frac{1}{F}\right]^{1/2} \tag{A-26}$$

$$r_H(t=\infty) = \left[1 - \frac{L}{H} + \frac{1}{F}\right]^{1/2} \tag{A-27}$$

From Eq. (A-19) we infer that the flow will enter Stage 3 only if

$$F \geq \left(1 - \frac{L}{H}\right)^{-1} \tag{A-28}$$

which, through (A-26), insures that $r_0 \geq 0$, and, through (A-27), that $r_H \leq 1$. Note that in the limit $F \to \infty$, the free surface forms an inner cylinder of constant radius, $r_0 = r_H = (1 - L/H)^{1/2}$.

Finally, the steady-state limit of the angular momentum, Eq. (A-9), in this configuration can be shown to be

$$L_z(t = \infty) = \frac{1}{4}\left[1 - \left(1 - \frac{L}{H}\right)^2 - \frac{1}{3F^2}\right] \tag{A-29}$$

We close by noting that all the expressions given above for the limiting condition of solid-body rotation agree with those derived by Gerber.[22,23]

Appendix B

FINITE DIFFERENCE EQUATIONS FOR THE AZIMUTHAL VELOCITY

When the differencing scheme described in Section 2 is applied to Eq. (3), the following tridiagonal system of equations results:

$$A_j v_{j+1}^{i+1} + B_j v_j^{i+1} + C_j v_{j-1}^{i+1} = D_j \tag{B-1}$$

where

$$A_j = \frac{\Delta t}{\Delta r}\left[\frac{u_j^{i+1}}{4} - \frac{1}{2Re}\left(\frac{1}{\Delta r} + \frac{1}{2r_j}\right)\right]$$

$$B_j = 1 + \frac{\Delta t}{2r_j} u_j^{i+1} + \frac{\Delta t}{Re}\left[\frac{1}{(\Delta r)^2} + \frac{1}{2r_j^2}\right]$$

$$C_j = -\frac{\Delta t}{\Delta r}\left[\frac{u_j^{i+1}}{4} + \frac{1}{2Re}\left(\frac{1}{\Delta r} - \frac{1}{2r_j}\right)\right]$$

$$D_j = v_{j+1}^{i}\frac{\Delta t}{\Delta r}\left[-\frac{u_j^{i}}{4} + \frac{1}{2Re}\left(\frac{1}{\Delta r} + \frac{1}{2r_j}\right)\right]$$

$$+ v_j^{i}\left[1 - \frac{\Delta t}{2r_j} u_j^{i} - \frac{\Delta t}{(\Delta r)^2 Re} - \frac{\Delta t}{2r_j^2 Re}\right]$$

$$+ v_{j-1}^{i}\frac{\Delta t}{\Delta r}\left[\frac{u_j^{i}}{4} + \frac{1}{2Re}\left(\frac{1}{\Delta r} - \frac{1}{2r_j}\right)\right]$$

Such systems are efficiently solved via a special adaptation of Gaussian elimination (Reference 25). Let

$$v_j^{i+1} = E_j v_{j+1}^{i+1} + F_j \tag{B-2}$$

which, when substituted into Eq. (B-1), requires that

$$E_j = -\frac{A_j}{B_j + C_j E_{j-1}} \tag{B-3a}$$

$$F_j = \frac{D_j - C_j F_{j-1}}{B_j + C_j E_{j-1}} \tag{B-3b}$$

These are applied at j = 2,3 . . . NJ - 1, with the starting values

$$E_1 = F_1 = 0$$

in accordance with Eq. (4a). Then, beginning with Eq. (4b), Eq. (B-2) is used to obtain the remaining velocities.

In Stage 3, the above procedure is modified since Eq. (4a) no longer applies. Let r_{j*} denote the first radial grid station that exceeds r_0; then only the points j* . . . NJ will be included in the algorithm described by Eq. (B-2) and (B-3). The starting values for E and F are inferred by requiring that a linear extrapolation from the velocities at r_{j*} and r_{j*+1} to r_0 should satisfy Eq. (20). The results are

$$E_{j*} = (r_{j*} - r_0) / (\Delta r + r_{j*} - r_0)$$

$$F_{j*} = r_0 \Delta r / (\Delta r + r_{j*} - r_0)$$

The values used for the relaxation parameter α in Eq. (5) are given in the table below.

Table B-1
Values of Velocity Relaxation Parameter

Free Surface Configuration (Figure 1)		α
Stages 1, 2b	$Z_0 \geq 0.2$	1.0
	$0.1 \leq Z_0 < 0.2$	0.5
	$Z_0 < 0.1$	0.2
Stage 3	$r_0 > 0$	0.4

These values, determined from experience, are not necessarily optimal. But with them, convergence was achieved typically within 2-3 iterations.


07-